MASSACHUSETTS INSTITUTE OF TECHNOLOGY

LINCOLN LABORATORY

REMOTE SENSING OF TURBINE ENGINE GASES

D.K. KILLINGER
N. MENYUK
A. MOORADIAN

Group 82

FINAL REPORT

TO THE

AIR FORCE ENGINEERING AND SERVICES CENTER

1 OCTOBER 1979 – 30 SEPTEMBER 1980

ISSUED 24 APRIL 1981

Accession For	
NTIS GRA&I	X
DTIC TAB	☐
Unannounced	☐
Justification	
By	
Distribution/	
Availability Codes	
Dist	Avail and/or Special
A	

LEXINGTON   MASSACHUSETTS

Contents

I. INTRODUCTION

This is the FY 80 final report on a laser remote sensing research program conducted by M.I.T. Lincoln Laboratory with support by the Department of the Air Force, in part with specific funding from the Air Force Engineering and Services Center. The effort is part of a larger on-going program at Lincoln Laboratory to develop laser remote sensing techniques for environmental monitoring and tactical detection and discrimination. Previous research conducted during FY 79 is documented in Final Report, ESD-TR-79-319/ESL-TR-80-09.[1]

The specific tasks which were performed during FY 80 for this research program consisted of the following: (1) continuation of feasibility demonstration of CO_2 TEA laser remote sensing system (described in Section II), (2) continuation of laboratory absorption measurements of CO, NO, and C_2H_4 (described in Section III), (3) initial laboratory investigation of suitability of laser remote sensing of hydrazine (described in Section VI), and (4) implementation of digital data acquisition and processing system (described in Section V). It should be noted that as originally proposed task (1) above included the demonstration of the laser remote sensing of selected pollutant gases in the atmosphere and in the exhaust from a stationary USAF jet aircraft. Because of the unavailability of such an aircraft during FY 80, this portion of task (1) was not conducted; instead, the preliminary development of a dual-laser DIAL system was performed (described in Section IV). This modification to the original Work Statement was given oral approval by the AFESC contracting officer. The remote sensing of the exhaust gases from the USAF jet aircraft will be conducted during FY 81 as stated in the FY 81 Work Statement.

Each of the tasks is described in the following sections of this report. Supportive documentation is included in the attached appendix.

II. FEASIBILITY DEMONSTRATION OF CO_2 TEA LASER REMOTE SENSING SYSTEM

Experimental studies were conducted to measure and demonstrate the feasibility of a CO_2 laser differential-absorption LIDAR (DIAL) system for the remote sensing of NO and C_2H_4 in the atmosphere. The studies were carried out using a compact mini-TEA CO_2 laser incorporated into a remote

101586-N-02

MINI-TEA
CO₂ LASER

SPECTROMETER

BEAM-EXPANDER
× 10

TOPOGRAPHIC
TARGETS

DETECTOR

TELESCOPE

ABSORPTION CELL → PYRO

PYRO

8085
CONTROLLER
(LeCroy)

CAMAC
A/D

TIMING/GATE
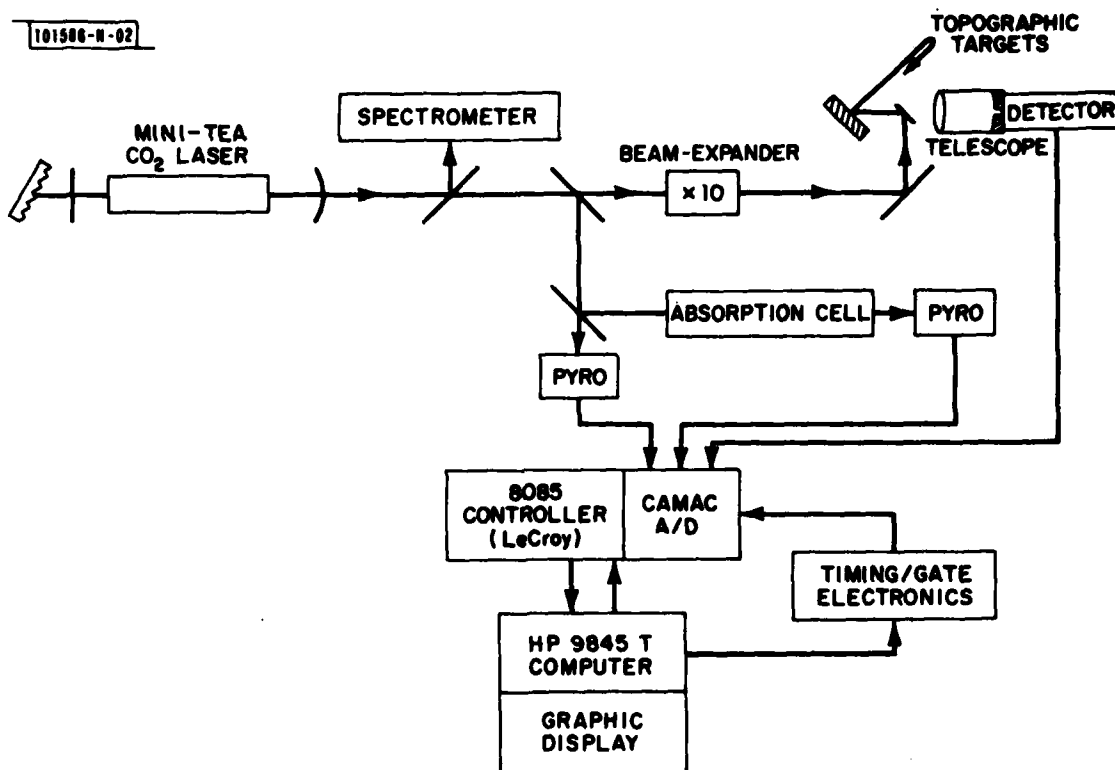ELECTRONICS

HP 9845 T
COMPUTER

GRAPHIC
DISPLAY

Fig. 1. Schematic of single-laser differential-absorption LIDAR system.

sensing DIAL system including transmitting and receiving optics, a detector, associated electronics, and a digital data acquisition system. This system is a modification to the DIAL system used previously for laser remote sensing measurements of atmospheric CO.[2] A schematic of the system is shown in Fig. 1. The output from a pulsed, tunable mini-TEA CO_2 laser served as the primary radiation source; laser characteristics were 20 mJ/pulse, 100 ns pulse length, and repetition rates of up to 500 Hz. A frequency-doubling crystal could be inserted into the beam for measurements in the 5-μm region. The laser radiation was sampled by means of beam splitters to provide spectral and intensity information for subsequent normalization and calibration of the DIAL signals.

The major portion of the beam was passed through a X10 beam expander and directed by steering mirrors toward topographic targets located outside the laboratory window. Backscattered radiation was collected by a 30-cm Cassegrain telescope and detected by either a HgCdTe or an InSb detector. The output signals were sampled by high-speed analog-to-digital converters and processed by a dual-computer data-acquisition system. Further information pertaining to the experimental apparatus and data acquisition system will be presented in a later section. Details of the actual experiments for the remote sensing of NO and C_2H_4 are presented in the next two sections.

2.1 Laser Remote Sensing of NO

The DIAL system was used to make single-ended remote sensing measurements of the atmospheric concentration of NO using 5.3-μm radiation; for these experiments, the 10.6-μm radiation from the mini-TEA CO_2 laser was frequency-doubled to 5.3-μm through use of a $CdGeAs_2$ crystal. The concentration of NO was deduced from differential-absorption of the laser backscatter from topographic targets at ranges up to 1.4 km. For the remote sensing of NO, frequency-doubled radiation of the 10.6-μm P(24) CO_2 transition was used as the on-resonance absorption frequency and doubled radiation from either the P(26) or the P(14) CO_2 transition was used as the off-resonance frequency. Details of the experimental apparatus, experimental procedure, and measurement results are presented in the appendix, which is a reprint of a journal article.[3]
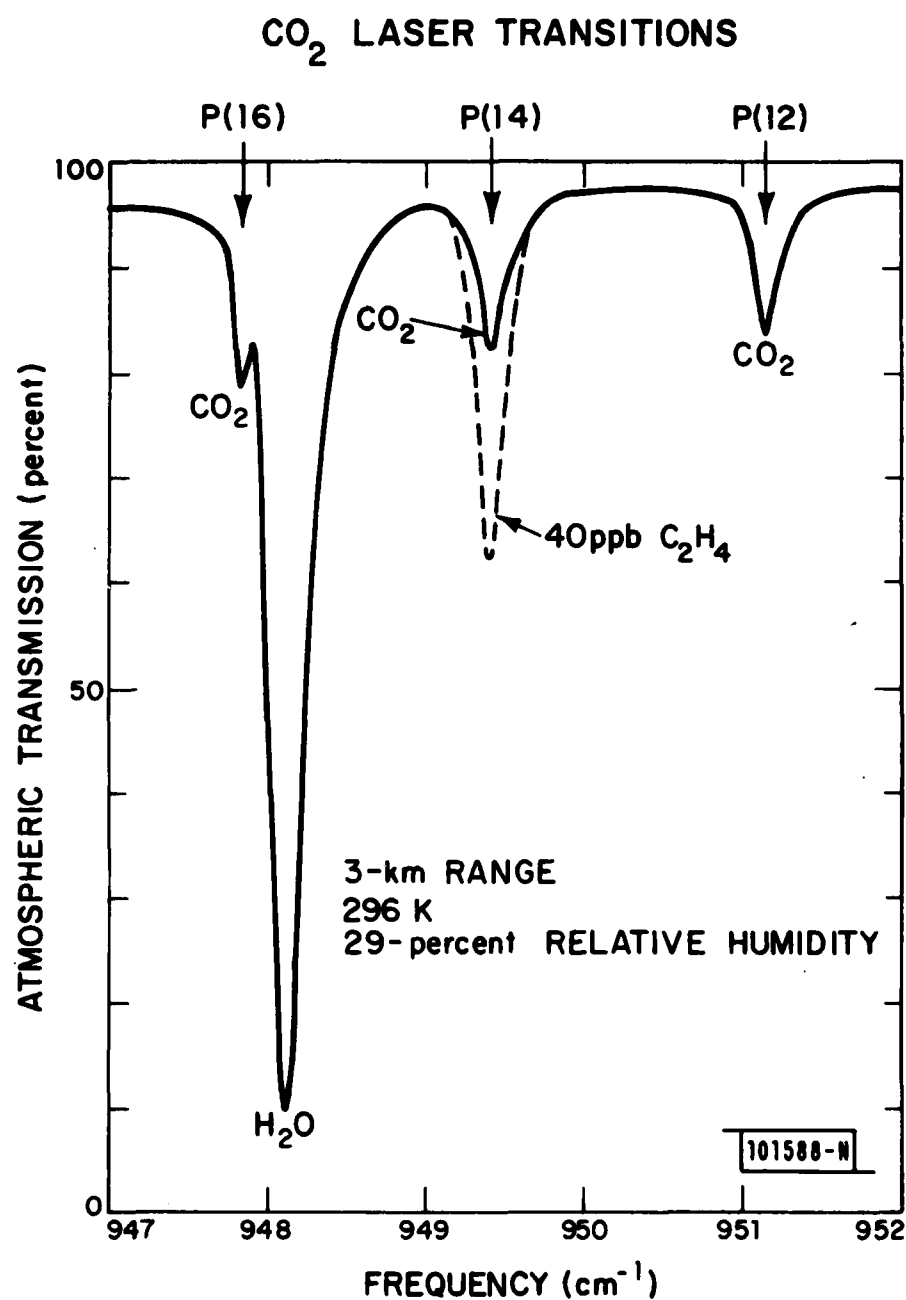
CO$_2$ LASER TRANSITIONS

Fig. 2.   Transmission of atmosphere near 10.5 μm showing increase in absorption due to C$_2$H$_4$.

4

As described in the appendix, the major results and conclusions based on the measurements are:

1) With the DIAL system, NO present in the exhaust of cars and trucks operating on a busy roadway was detected at path-averaged concentrations of 100-200 ppb (parts per billion) at ranges up to 500 m.

2) Uncertainties in these measurements were on the order of 40 ppb and were primarily due to temporal changes in the absorption background due to atmospheric water vapor.

3) The background interference due to water vapor was measured by the DIAL system. These results were compared to those predicted by the HITRAN atmospheric transmission computer program and significant deviations were noted; these deviations were primarily due to uncertainties in the laser transition frequencies and water vapor absorption line shape.

2.2 Laser Remote Sensing of C_2H_4

Laser remote sensing measurements of atmospheric C_2H_4 were conducted[4] through use of the single-laser DIAL system (Fig. 1). For the remote sensing of C_2H_4, the P(14) CO_2 laser transition near 10.5 μm was used as the on-resonance absorption frequency and the P(12) CO_2 laser transition was used as the off-resonance absorption frequency. This may be seen in Fig. 2, which shows the transmission of the atmosphere near 10.5 μm (950 cm^{-1}) and the increase in absorption due to the presence of C_2H_4 in the atmosphere. The concentration of C_2H_4 in the atmosphere is determined from the increased absorption of the P(14) LIDAR return from topographic targets compared to that of the P(12) line.

Using this system, the increase in C_2H_4 in the atmosphere was detected over a busy traffic roadway at a range of 500 m. The results, which indicate the increase in C_2H_4 due to automobile exhaust as the traffic over the roadway increased, are shown in Fig. 3. Measurements on other days yielded peak concentrations of C_2H_4 as high as 230 ppb. The concentration was observed to be quite dependent on wind direction and local weather conditions.
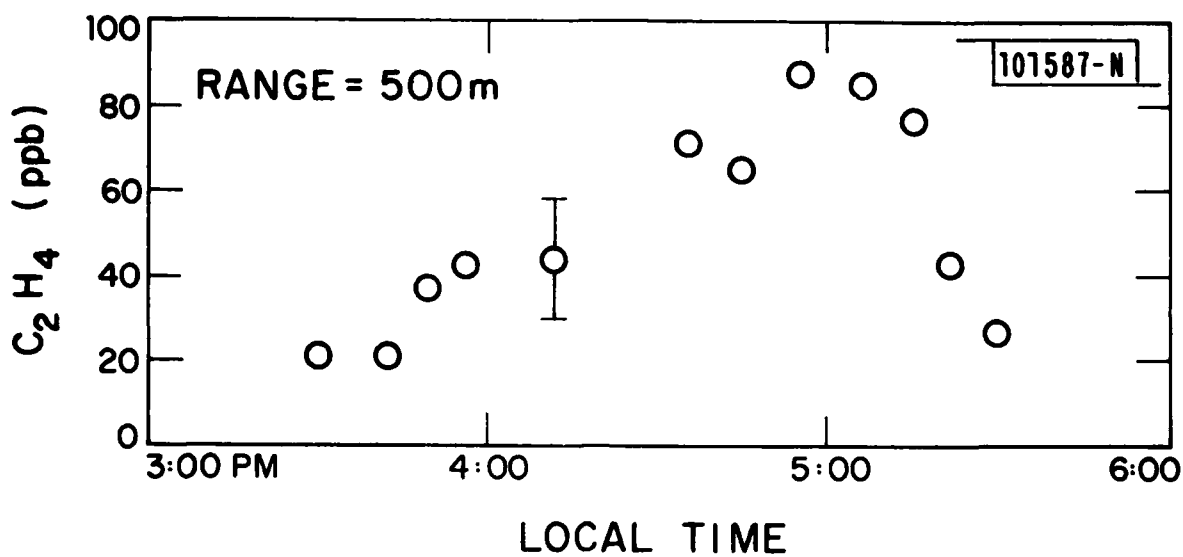
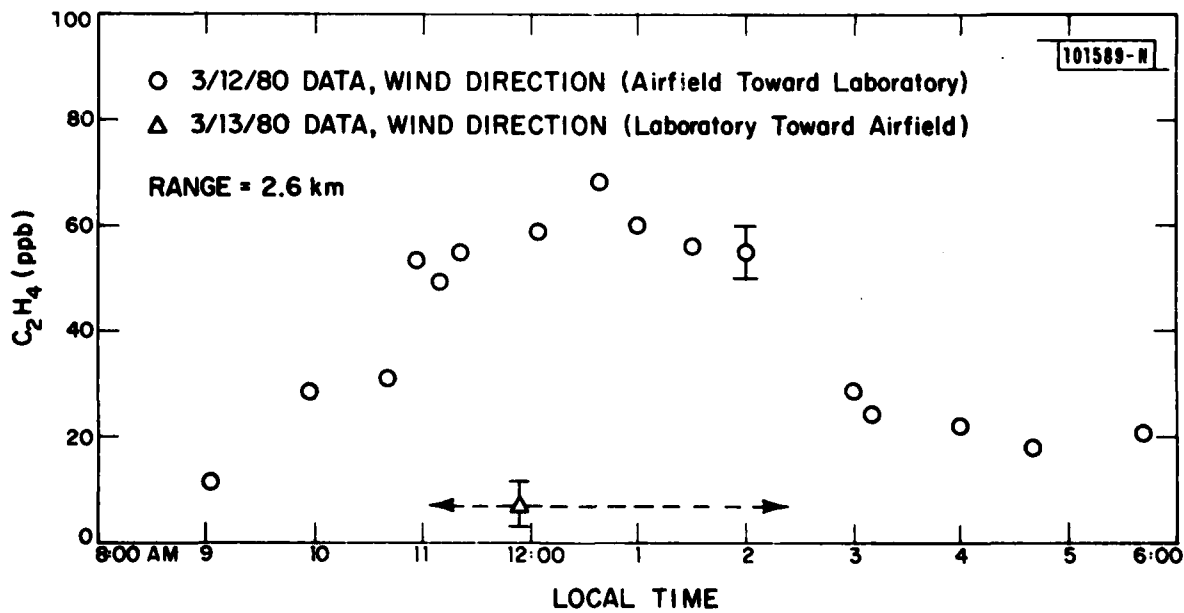Fig. 3. DIAL measurements of C_2H_4 for a path encompasssing a major traffic roadway.

Fig. 4. DIAL measurements of C_2H_4 for a path encompassing a busy airfield.

Figure 4 shows the diurnal variation of C_2H_4 measured over an adjacent airfield (Hanscom AFB) using the Lincoln Laboratory Flight Facility as a topographic target (range 2.7 km). The results indicate an ambient background concentration of C_2H_4 on the order of 10 ppb with increases up to 70 ppb, probably due to aircraft exhaust or fuel emission; for the upper curve shown, the wind direction was from the airfield toward our laboratory. Of interest is the result that little C_2H_4 was observed on the next day, when the wind direction shifted and blew from the laboratory toward the airfield.

The results shown in Fig. 4 also indicate an uncertainty in the measurements on the order of 10 ppb. Such error is due to temporal variation in the background off-resonance LIDAR signal. It is anticipated that these errors may be reduced through use of a dual-laser DIAL system.

III. LABORATORY ABSORPTION MEASUREMENTS OF CO, NO, AND C_2H_4

The absorption characteristics of gaseous CO, NO, and C_2H_4 were investigated. In particular, the absorption coefficients at the associated CO_2 laser transition frequencies were measured using the experimental setup as shown in Fig. 1 and subsequently compared to previous measurements by other investigators.[5,6] The measurements agreed with these other observations within ± 10%, which is within the experimental uncertainty due to the tuning range of the atmospheric-pressure-broadened mini-TEA CO_2 laser. For completeness, the pertinent absorption characteristics of CO, NO, and C_2H_4 useful in CO_2 laser remote sensing measurements are given in Table I along with the anticipated background atmospheric attenuation, β, appropriate for the U. S. Standard Atmosphere model.[7] The values presented for CO, NO and C_2H_4 are given in terms of the absorption strength, $S(cm^{-1}/molecule/cm^2)$, and the half-width at half-maximum pressure broadened linewidth, $\alpha(cm^{-1})$, at 760 Torr. The absorption coefficient, $\sigma(cm\ atm)^{-1}$, is also given in Table I. σ is related to S and α by

$$\sigma = \frac{S\,\alpha\,L}{\pi\,[\Delta\nu^2 + \alpha^2]} \qquad , \tag{1}$$

Table I: Absorption Characteristics of CO, NO, and C₂H₄ at Selected CO₂ Laser Transitions

CO₂ Laser Transition		Gaseous Absorption Characteristics					Atmospheric Attenuation
Line	$\nu(cm^{-1})$	Transition	ν (cm^{-1})	S $(cm^{-1}/molecule/cm^2)$	α (cm^{-1})	σ $(cm\ atm)^{-1}$	β $(km)^{-1}$
		(CO)					
2νP(24)	2086.327	P(14)	2086.325	0.172×10^{-18}	0.060	22.63	0.195*
2νP(26)	2082.558	—				0.0	0.050
2νR(18)	2154.605	R(2)	2154.598	0.254×10^{-18}	0.078	25.70	0.231*
2νR(16)	2151.97	—				0.0	0.036
		(NO)					
2νP(24)	1881.098	R(1/2)₁/₂	1881.0398	0.177×10^{-19}	0.062	1.2	0.592
2νP(26)	1877.378	—				0.0	0.706
2νP(14)	1884.768	—				0.0	0.555
		(C₂H₄)					
P(14)	949.48	28,1,27→28,2,27				32.14	0.122
P(12)	951.193	—				4.3	0.116

*Includes attenuation due to atmospheric background concentration of 75 ppb of CO (reference 7).

8

where $\Delta\nu$ is the difference in frequency between the radiation and the absorbing transition, and L is Loschmidt's number, 2.48×10^{19} molecules/cm^3; L is the concentration of molecules in the atmosphere at 20°C and standard pressure. The attenuation of an optical beam is given by the equation

$$I = I_0 e^{-\sigma NR} \qquad (2)$$

where R is the distance in cm traveled by the beam, N is the concentration of the gas in fractions of a standard atmosphere, and I is the intensity of the beam.

It should be noted that while the laboratory measurements served to verify the values given in Table I, the laser remote sensing system is self-calibrating. That is, known concentrations of CO, NO, or C_2H_4 are used in the absorption cell (Fig. 1) for simultaneous comparison of the differential-absorption values with that of the DIAL returns.

IV. PRELIMINARY DEVELOPMENT OF DUAL-LASER DIAL SYSTEM

During the initial investigation into laser remote sensing of CO, NO, and C_2H_4 using a single-laser DIAL system, it was evident that a significant part of the measurement error was due to short- and long-term temporal changes in the background absorption of the atmosphere. These changes cannot be averaged out in view of the large-scale temporal changes which occur in the atmosphere within the time scale of the measurements. Such errors were measured to be on the order of 10-20%, depending upon atmospheric wind and weather conditions.

In order to reduce such error-causing effects, a dual-laser DIAL system was designed and implemented. This system permits the nearly simultaneous transmission of the on-resonance and off-resonance LIDAR beams so that the differential-absorption signal may be measured on a short temporal basis. This is in contrast to the typical single-laser DIAL system technique of alternating the single laser between the on-resonance transition and the off-resonance transition every 30 s or so. The dual-laser DIAL system implemented was similar to that shown in Fig. 1 except two mini-TEA

CO_2 lasers are used. A schematic of this system is shown in Fig. 5 and a photograph of the system is shown in Fig. 6. The two lasers are pulsed separately with a time delay which is typically 35 µs. This provides for temporal separation of the two LIDAR returns.

Preliminary measurements with this dual-laser DIAL system have indicated an overall improvement in the resultant measurement accuracy compared to that of a single-laser DIAL system. Future studies are planned to quantify these improvements.

V. IMPLEMENTATION OF DIGITAL DATA ACQUISITION AND PROCESSING SYSTEM

The experiments reported for the laser remote sensing of CO and NO were conducted using an analog data processing system involving boxcar integrators, analog ratiometers, and chart recorders. Due to the low duty cycle of the DIAL system, ($\sim 10^{-5}$), corresponding to the laser pulse-width (100 ns) multiplied by the pulse repetition frequency, boxcar integrators are severely limited when used for signal processing of the input DIAL signals.

A more suitable system is a digital data acquisition system consisting of fast analog-to-digital converters linked to a dedicated minicomputer. Such a system has been implemented and a photograph of this system is shown in Fig. 7. The system involves A/D CAMAC modules interfaced to a LeCroy 3500 Computer, with subsequent data transferred to a Hewlett Packard 9845T Computer for further statistical analysis. Specific details are: (1) CAMAC A/D Converters; LeCroy #2249SG, (2) Timing Gate Modules; Ortec #416A gate and delay generator, and BNC #8010 pulse generator, (3) Signal Processing Computer: LeCroy 3500M data acquisition computer with CAMAC mini-crate, 8085 CPU processor, GPIB IEEE-488 output, and CP/M FORTRAN programming, and (4) Statistical Analysis Computer: Hewlett Packard 9845T computer with graphics capability, graphics thermal printer, and HPIB IEEE-488 interface.

The LeCroy 3500 system is used to record the LIDAR, absorption cell, and laser pulse power signals, normalize the input signals to the laser pulse power, check for possible laser misfires, and form the histogram of these input signals. Data can be collected by the LeCroy 3500 at a rate

TARGET

BEAM STEERING MIRROR

M

HgCdTe DETECTOR

M

BEAM EXPANDER

M

LASER NO. 2

BS

BS

ABSORPTION CELL

PYRO DETECTOR NO. 2

DELAYED TRIGGER

PYRO DETECTOR NO. 1

LASER NO. 1

M

TIMING CIRCUITS

CAMAC A/D

COMPUTER (LeCroy 3500)

DISPLAY
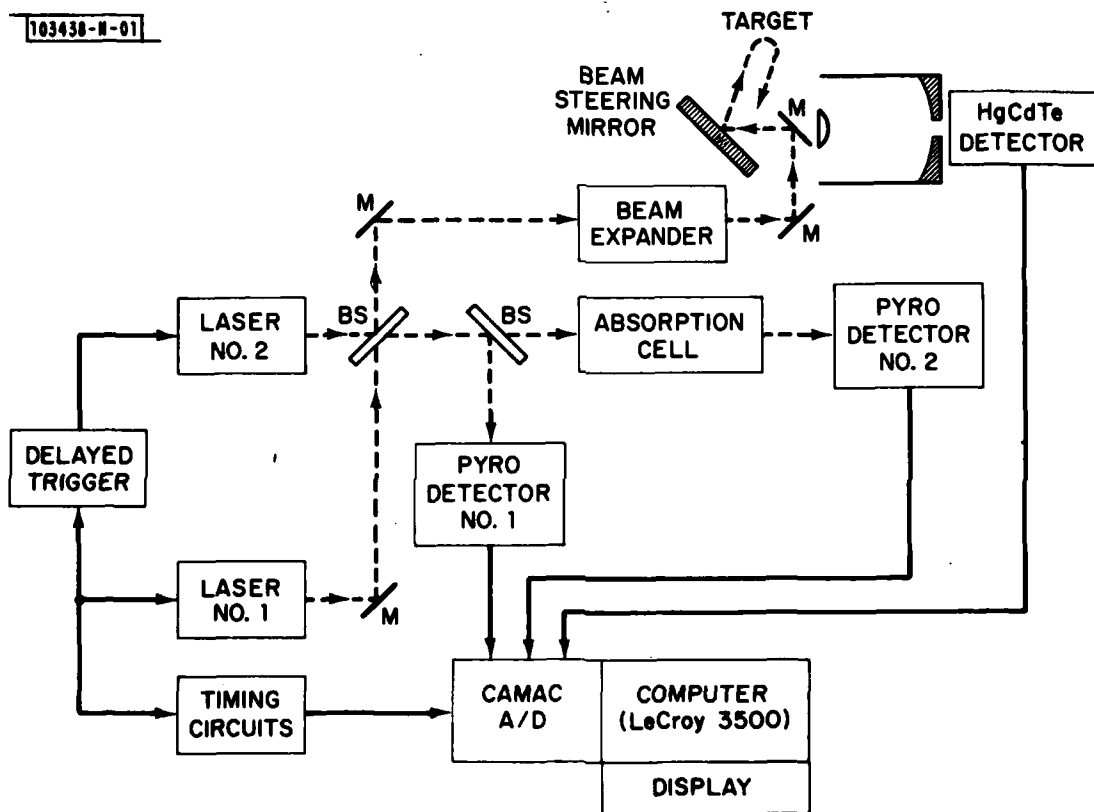
Fig. 5.   Schematic of dual-laser DIAL system.

11

107453-S
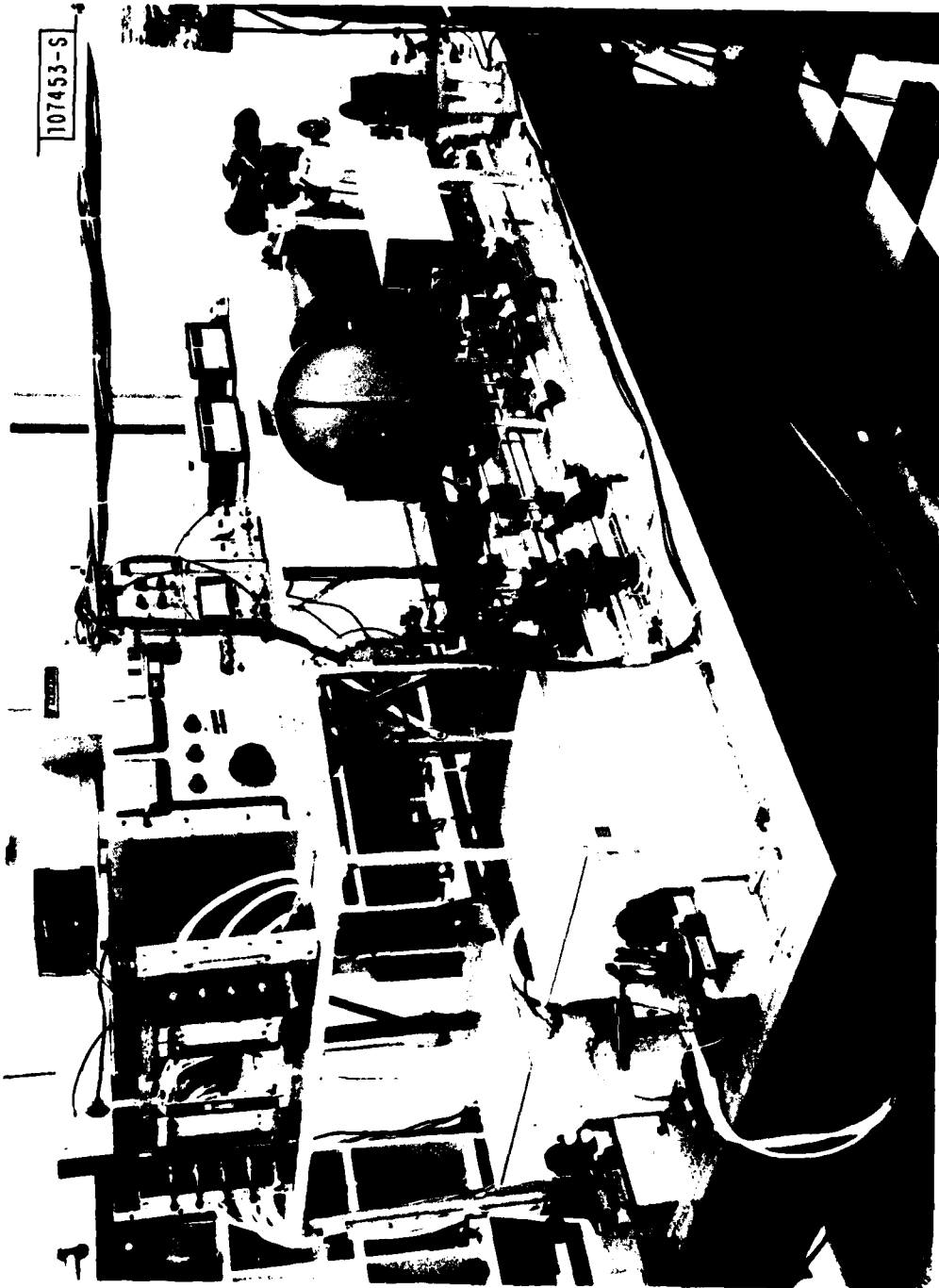
Fig. 6. Photograph of dual-laser DIAL system.

12

Fig. 7. Photograph of digital data acquisition system.

13

1000 PULSES, AV = 1.006, S.D. = 4.112% OF AV

1000 PULSES, AV = 0.860, S.D. = 22.349% OF AV

1000 PULSES, AV = 0.616, S.D. = 4.801% OF AV

1000 PULSES, AV = 0.440, S.D. = 22.578% OF AV

NORMALIZED INTENSITY

Fig. 8. Typical histogram of LIDAR returns and absorption cell signals. The 10.5-μm P(12) and P(14) CO_2 laser transitions are used for the remote sensing of C_2H_4.

of up to a few hundred hertz. After compiling a few thousand pulses, the data are transferred by the IEEE-488 data-bus from the LeCroy 3500 to the HP9845T computer. A statistical analysis (mean, standard deviation) is performed by the HP9845T and a linear or logarithmic graphical display is produced. An example of such output is shown in 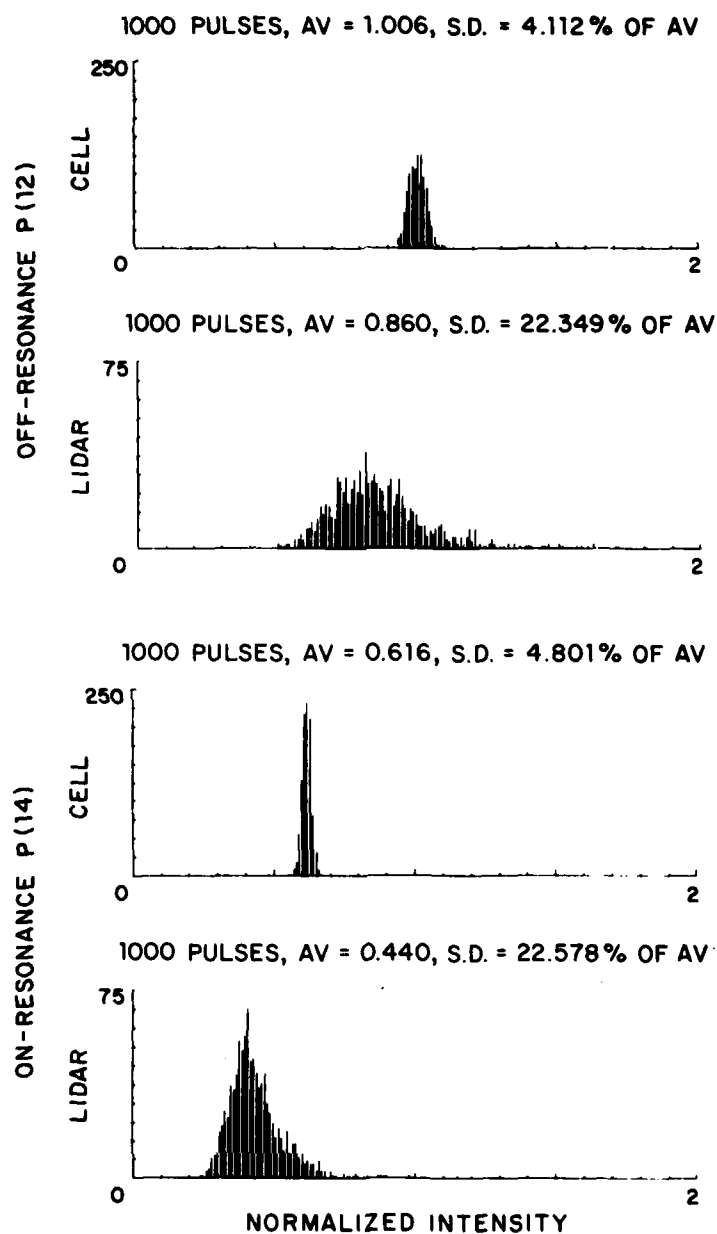Fig. 8. As evident in Fig. 8, the statistical spread of the LIDAR returns is much greater than that associated with the absorption cell and is indicative of the effects of atmospheric turbulence and target scintillation.

It should be noted that the use of the digital data acquisition system described above has resulted in a substantial improvement in the DIAL measurement accuracy. This improvement, compared to that of the previously used analog system (boxcar integrators), has been approximately proportional to the square root of the number of pulses integrated. Further studies to better quantify this result will be conducted.

VI. INITIAL LABORATORY INVESTIGATION OF SUITABILITY OF LASER REMOTE SENSING OF HYDRAZINE COMPOUNDS

The suitability of a CO_2 DIAL system for the remote sensing of hydrazine, unsymmetrical dimethyl hydrazine (UDMH), and monomethyl hydrazine (MMH) in the atmosphere has been investigated. The initial phase of this effort included: (1) the determination of the appropriate CO_2 laser transitions for remote sensing of the hydrazine compounds, (2) theoretical estimates of the expected detection range of such DIAL measurements, and (3) the laboratory measurement and verification of the differential-absorption coefficients in a DIAL configuration. The results are detailed in the following sections and basically indicate that path integrated concentrations of hydrazine, UDMH, and MMH on the order of tens of parts per billion should be observable for detection ranges of up to several kilometers.

6.1 Preferred CO_2 Laser Frequencies for Remote Sensing of Hydrazine Compounds

The choice of CO_2 laser frequencies to be used for the remote sensing of the hydrazines includes consideration of: (1) those CO_2 frequencies

15

obtainable with the mini-TEA CO_2 lasers, (2) the differential-absorption of the hydrazine compounds at these frequencies, and (3) the atmospheric transmission and interference from other atmospheric species at these frequencies.

With our mini-TEA CO_2 lasers, single line radiation is obtainable from the P(8) to P(36) and the R(10) to R(34) lines of the (00°1) - (10°0) transition near 10.6 μm and from the P(10) to P(34) and the R(10) to R(34) lines of the (00°1) - (02°0) transitions near 9.4 μm.[8]   The frequencies chosen must be limited to these lines. The differential-absorption coefficients of hydrazine, UDMH, and MMH at the CO_2 laser transition frequencies are available from measurements obtained by Loper et al.[9] using a tunable low-pressure CW CO_2 laser.

The atmospheric transmission and possible interferences of other molecular species are obtained from the AFGL tapes of McClatchey et al.[7] Among the potential interfering species, ethylene and ammonia are of particular importance. Ethylene exists as a trace element in the atmosphere and is present in vehicle exhausts. Average concentration levels in excess of 60 parts per billion (ppb) have been observed over an airbase (see Section 2.2). Ammonia is both an atmospheric trace element with a normal concentration[10] between 2 and 20 ppb and a reaction product of hydrazine decomposition. Absorption coefficients of both ammonia and ethylene have been measured at CO_2 laser frequencies and are available in the literature.[5,6,10]

Using the above considerations, CO_2 laser frequency pairs were chosen to yield as large a differential-absorption as possible consistent with minimal interference effects from either ethylene or ammonia. It is desirable to choose the frequency pairs close together in order to maximize the mutual coherence[11,12] of the two laser beams. However, this is difficult for both UDMH and MMH. Explicit choices are discussed in turn for each of the hydrazines.

a. **Hydrazine**

Significant absorption of hydrazine[9] occurs only in the 10.6-μm band of

16

CO_2 laser transitions. CO_2 laser wavelengths longer than the P(30) line are eliminated by the extremely high NH_3 absorption. The most suitable laser transition pair is the P(22) transition at 10.611 μm as the high-absorption line and the P(28) transition at 10.674 μm as the low-absorption line. The corresponding absorption coefficients[9] are 5.41 and 2.17 (cm atm)$^{-1}$, respectively, yielding a differential-absorption of $\Delta\sigma$ = 3.24 (cm atm)$^{-1}$. With this choice, the frequencies are closely spaced, the differential-absorption levels of both C_2H_4 and NH_3 are seen to be smaller than that of hydrazine by over an order of magnitude, and the atmospheric transmittance level is acceptable at both frequencies. The corresponding absorption values are given in Table II along with the background atmospheric attenuation, β, for a U. S. Standard Atmosphere.[7]

b. UDMH

The choices of laser transition pairs for DIAL measurements of UDMH are extremely limited. As previously determined,[9] the absorption coefficient of UDMH in the 9.4-μm CO_2 laser band is approximately 1.5 (cm atm)$^{-1}$, with very little variation within the R and P branches. Significant absorption occurs in the 10.6-μm band only for the longer wavelengths of the P branch, rising from ~ 1 to near 3 (cm atm)$^{-1}$ between the P(28) and P(36) laser transitions of the 10.6-μm band. There is virtually no absorption of UDMH within the R branch of the 10.6-μm band [σ ~ 0.05-0.2 (cm atm)$^{-1}$].

Absorption interferences occur in the 10.6-μm P branch due to NH_3 absorption lines. Between the P(32) and P(36) transitions, NH_3 absorption is a factor of 3 to 7 times greater than that of UDMH. Although NH_3 is only a minor product of UDMH decomposition, this large a relative absorption level coupled with the possible presence of even small amounts of ambient NH_3 effectively allows only the P(28) or P(30) to be used for the high-absorption transitions. The UDMH absorption coefficients for these lines are 1.11 and 1.45 (cm atm)$^{-1}$, respectively.

No other line could be found within the P branch of the 10.6-μm CO_2 laser band which, in conjunction with either the P(28) or P(30) transition, would yield a differential absorption level which was of the

Table II: Relevant Absorption Parameters for the Remote Sensing of the Hydrazines.

CO_2 Laser Transition	Wavelength (μm)	Absorption Coefficients $(cm\text{-}atm)^{-1}$			Atmospheric Attenuation $\beta(km)^{-1}$
		Hydrazine	NH_3	C_2H_4	
P(22)	10.611	5.41	0.045	1.09	0.1142
P(28)	10.675	2.17	0.36	1.30	0.0976
Differential Absorption		3.24	-0.315	-0.21	
		UDMH	NH_3	C_2H_4	
P(30)	10.696	1.45	0.86	1.63	0.0907
R(10)	10.318	0.05	0.78	1.51	0.1142
Differential Absorption		1.40	0.06	0.12	
		MMH	NH_3	C_2H_4	
R(30)	10.182	1.36	0.029	0.56	0.1137
R(18)	9.282	0.23	0.13	0.61	0.1418
Differential Absorption		1.13	-0.10	-0.05	

18

order of unity and significantly discriminated against both NH_3 and C_2H_4.
In order to do so, it was necessary to choose the low-absorption line from
within the R branch of the 10.6-μm band. Thus, the most suitable laser
transition pair appears to be the P(30) line as the on-resonance transition
and the R(10) line as the off-resonance transition, both in the 10.6-μm
band. The relevant absorption values are given in Table II.

c. __MMH__

Difficulties in finding a suitable pair of CO_2 laser transitions for
remote sensing of MMH are even greater than for UDMH. There is little MMH
absorption anywhere within the 9.4 μm band, while absorption value varia-
tions within the available transition lines of the 10.6-μm band are ex-
tremely small. The single exception is the R(8) line, for which $\sigma = 3.5$
$(cm\ atm)^{-1}$ compared to values near unity for neighboring transitions. How-
ever, the CO_2 mini-TEA lasers do not operate on this line; in addition, the
absorption coefficient of NH_3 at the frequency of this transition is ex-
tremely large, namely 25.8 $(cm\ atm)^{-1}$. Therefore it was necessary to con-
sider transition pairs involving CO_2 laser lines in different bands. It
was found that of all the 9.4-μm band transitions only the R(18) transition
will yield a sufficiently low C_2H_4 differential-absorption level to serve
as a suitable off-resonance line. Further consideration established the
R(30) line in the 10.6-μm band as the preferred on-resonance MMH-absorption
transition. The absorption values for this transition pair are also in-
cluded in Table II.

6.2 Calculation of Minimum Detectable Concentrations of Hydrazine Compounds

The differential absorption values for the hydrazines as given in
Table II are seen to be small; this is particularly true for UDMH and MMH.
To establish if remote sensing is feasible under these circumstances, cal-
culations were made of the expected DIAL detection sensitivity as a func-
tion of range for each of the hydrazines.

19

In general, one of two possible approaches is usually taken to determine the minimum observable concentration, n_{min}, of a trace specie as a function of range, R. The first establishes the limitation by setting the difference in the backscattered returns at the two frequencies equal to the noise signal. The second approach assumes a limitation in the ability to distinguish changes in the difference between the return signals at the two frequencies below some predetermined value. We will consider the effects of both limitations for each of the hydrazines. The basis for the calculations have been given in a previous Lincoln Laboratory report[1] and will not be repeated here.

For the case in which the difference in the return signals, ΔP_r, is set equal to the noise signal, P_n, it may be shown[1] that

$$n_{min} \simeq \frac{\pi R \tau P_n}{2 \rho K A E \Delta\sigma \exp(-2\beta R)} \quad , \tag{3}$$

where $\Delta\sigma$ is the difference in the molecular absorption coefficients of the trace specie at the two DIAL wavelengths, P_n is the dark-current limited noise signal, R is the range, β is the atmospheric extinction coefficient in the absence of the detected molecule, A is the area of the receiving telescope, ρ is the reflectivity of the topographic target, E is the LIDAR transmitted energy per pulse, and τ is the pulse length. To evaluate Eq. (3), one may use parameter values appropriate to our DIAL system of $P_n = 2 \times 10^{-8}$ W, $\rho = 0.1$, K = 0.1, A = 600 cm^2, and $E/\tau = 10^5$ W. Then

$$n_{min} = \frac{(5 \times 10^{-9})R}{\Delta\sigma \exp(-2\beta R)} \quad , \tag{4}$$

where R is the range in km, $\Delta\sigma$ is in units of (cm atm)$^{-1}$, and n_{min} is in units of atmospheres. To express n_{min} directly in parts per billion Eq. (4) is rewritten as,

$$n_{min} \, (ppb) = \frac{5R}{\Delta\sigma \exp(-2\beta R)} \quad . \tag{5}$$

20

Equation (5) represents the maximum sensitivity achievable with a single laser pulse pair for the case of ΔP_r equal to the noise in the system.

Under high signal-to noise-conditions, a more valid approach is to establish the minimum relative difference in the two differential-absorption LIDAR returns ($\Delta P_r/P_r$) which can be measured. Assuming that value to be 1%, this leads to a minimum detectable concentration[1] of

$$n_{min} \text{ (ppb)} = \frac{50}{\Delta\sigma R} \quad , \tag{6}$$

subject to detector noise limitations and range restrictions.

Using Eqs. (5) and (6), the minimum detectable concentrations of the hydrazines have been determined as a function of range for a single pulse pair. The resulting values for hydrazine, UDMH and MMH are shown graphically in Figs. 9, 10, and 11, respectively. The frequency pairs considered and the values of $\Delta\sigma$ and β for the U.S. Standard Atmosphere[7] used in the evaluation are given in Table II. In addition, the effect on detection sensitivity of having greater or lesser amounts of water vapor in the atmosphere, as represented by the mid-latitude summer and mid-latitude winter atmospheres,[7] respectively, is also shown in these figures. As seen in the figures, the detection limit at close ranges is due to the 1% minimum set for $\Delta P_r/P_r$ in Eq. (6) and the limit at longer ranges is due to the system noise limitation as given in Eq. (5).

The results shown in Figs. 9-11 indicate that remote sensing of the hydrazine-related molecules in concentrations of the order of 10-100 ppb is feasible at ranges up to 5 km. These results can be improved by averaging over several pulses. However, the predicted $\sqrt{N}$ improvement, where N is the number of pulses averaged, is at best limited to the number of pulses that can be measured in a few seconds. Beyond that period the accuracy of the measurement is limited by long-term temporal atmospheric variations.[4] Using digital signal processing techniques, detection ranges on the order of 10-20 km should be feasible for concentrations on the order of 10 ppb.
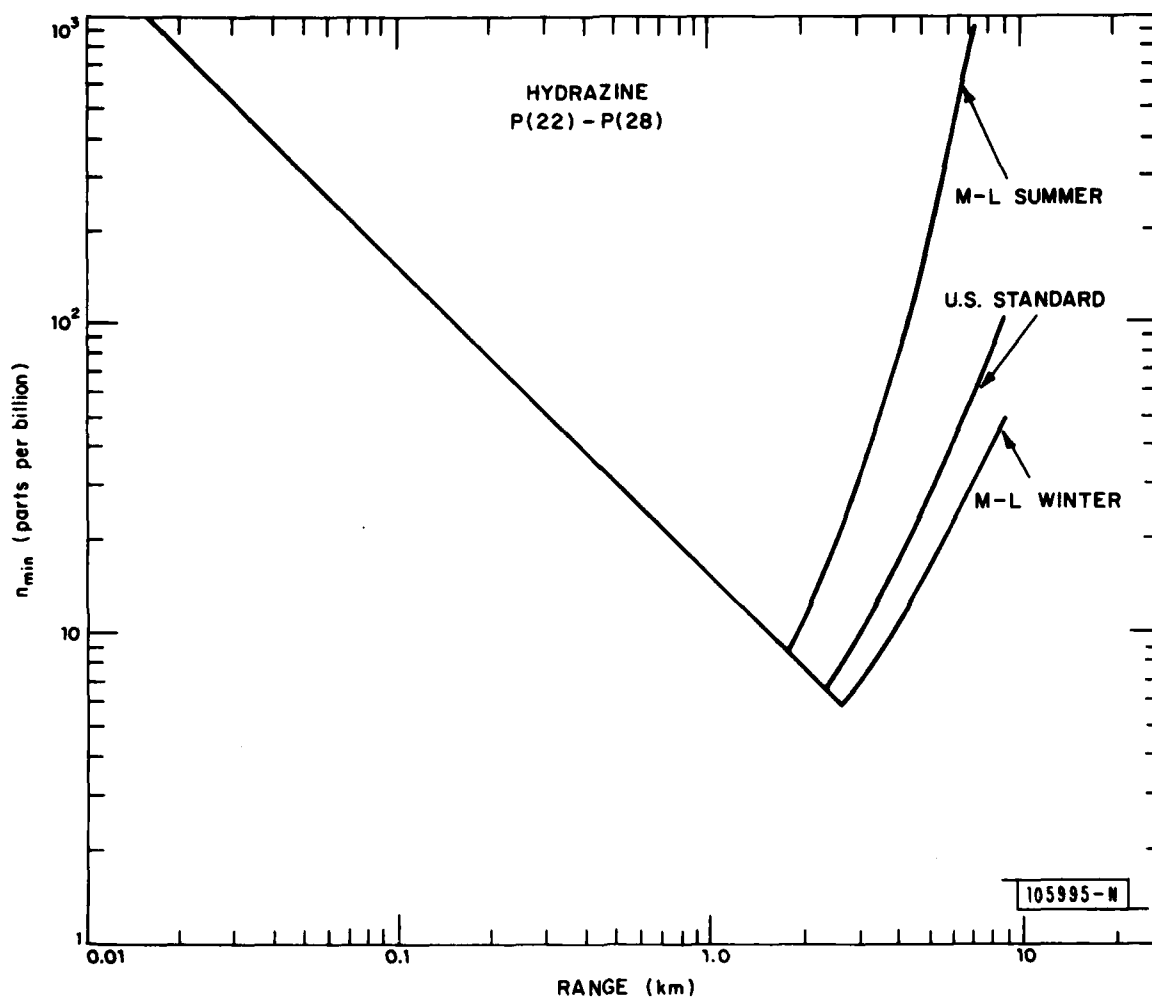
21

Fig. 9. Minimum detectable average hydrazine concentration by topographic reflection as a function of range using a single 10-mJ pulse.
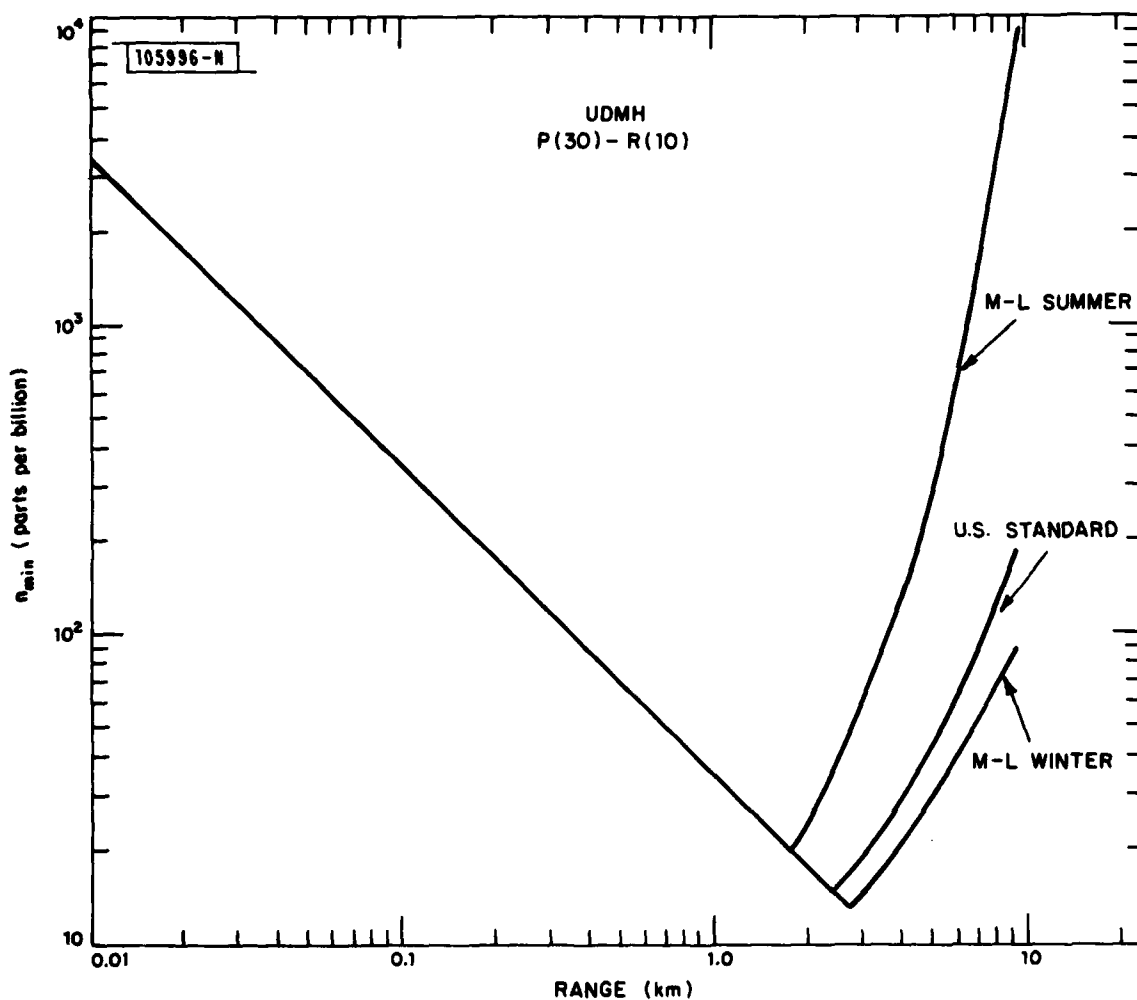
Fig. 10. Minimum detectable average unsymmetrical dimethylhydrazine (UDMH)
concentration by topographic reflection as a function of range using a
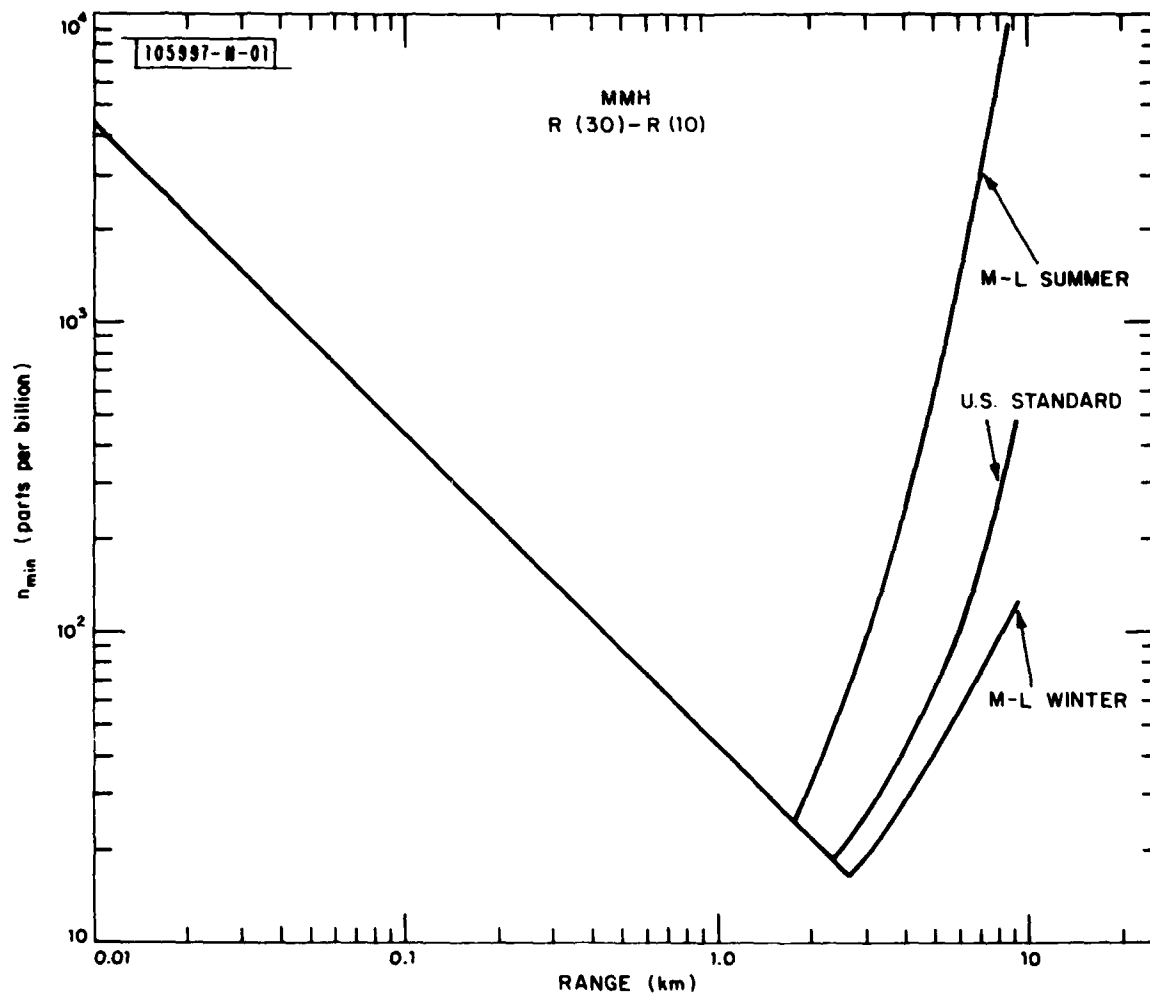single 10-mJ pulse.

Fig. 11.   Minimum detectable average monomethylhydrazine (MMH) concentration by topographic reflection as a function of range using a single 10-mJ pulse.

6.3 Laboratory Absorption Measurements of Hydrazine, UDMH, and MMH

The published absorption measurements of the hydrazines were obtained by Loper et al.[9] using a low-pressure CW CO_2 laser. Such lasers generally have narrow gain-bandwidths ($\sim$ 100 MHz) capable of supporting only a single longitudinal mode, which is located at or very near line center. However, to achieve the high peak CO_2 laser powers required for remote sensing over long ranges, the coherent radiation is usually provided by a pulsed CO_2 TEA laser operating at or near atmospheric pressure. Such lasers have collision broadened gain-bandwidths of the order of 1 GHz and generally operate on more than one longitudinal mode within a single transition line. Each mode operates at a slightly different frequency, and a small degree of tunability exists within each line. Given these circumstances, it is not obvious that the absorption coefficient of a given molecule for a particular CO_2 laser line, as observed with a low-pressure laser, will agree with the value obtained using a TEA laser operating on the same line.

Therefore, to determine if the results based on the low-pressure laser measurements which were used in the calculations for the expected detection ranges of the hydrazines are applicable to the present remote sensing system, absorption measurements were repeated for the chosen frequency pairs using the mini-TEA CO_2 lasers of our dual-laser LIDAR system. The technique used and the experimental results are discussed below.

a. Experimental technique

The dual-laser system shown in Fig. 5 was used to measure the absorption coefficients of the hydrazines in the laboratory. The system consisted of mini-TEA laser no. 1 firing on the line corresponding to the on-resonance absorption transition followed by mini-TEA laser no. 2 firing 50 µs later on the line corresponding to the off-resonance transition. Portions of both laser beams followed identical paths after passage through a beam splitter. The beams were further split, with one portion going to pyroelectric detector no. 1 which served as a normalizing beam. The remainder of the beams passed through a Pyrex absorption cell with BaF_2
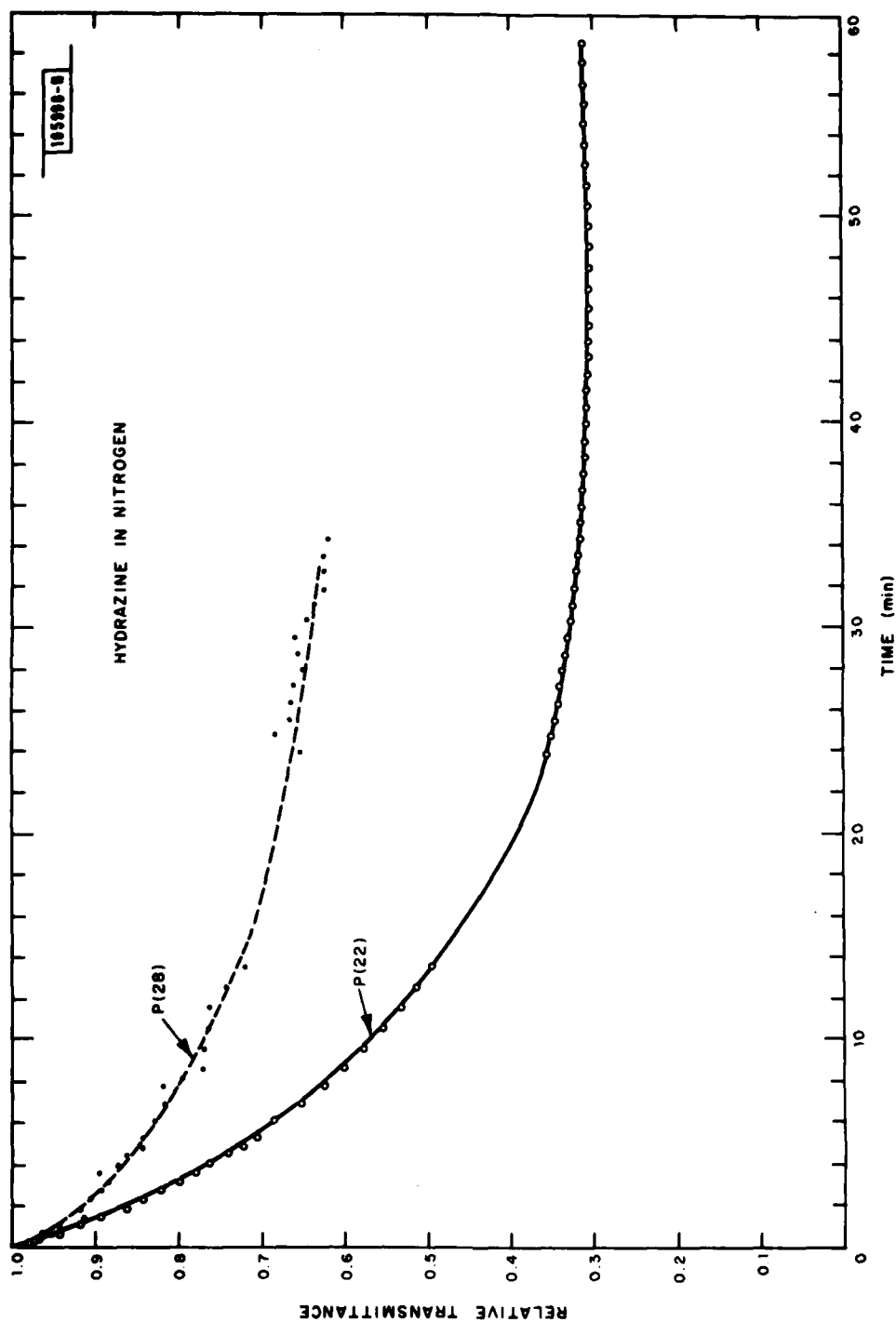
Fig. 12. Time variation of relative transmittance of 10.6-μm P(22) and 10.7-μm P(28) radiation through absorption cell containing nitrogen after inserting 1.6 μℓ of liquid hydrazine.

having a 2.54-cm diameter and a 31-cm length which initially contained
either air or nitrogen at atmospheric pressure and to which a known amount
of the hydrazine was added. The beam transmitted through the cell was
recorded by detector no. 2. The detector outputs along with gating cir-
cuitry then went to a computer system where each individual pulse was
normalized. The normalized pulses from each laser were averaged over a
preset number of pulses.

The 100% transmittance level through the absorption cell was estab-
lished by taking the values of the normalized laser beams, averaged over
a thousand pulses, after passage through the absorption cell containing
pure nitrogen at atmospheric pressure. A known volume of a hydrazine
compound in liquid form was then inserted into the cell and the laser beam
transmittance observed as a function of time. Initial values of the
average relative transmittance were taken for every 100 pulses; after the
rate of change declined, values were taken of the average of 500 pulses
from each laser. Nitrogen was used as the mixing gas to provide collision
broadening comparable with that of air and to be consistent with the meas-
urements of Loper et al.[9]

In addition to the above, a similar set of measurements was performed
with each of the hydrazines, but using air rather than nitrogen as the mix-
ing gas. Since the hydrazines are strongly subject to oxidation effects,[13-15]
these measurements cannot be used for direct measurement of the absorption
coefficients. However, the results are of considerable interest as they
point out additional problems which will be encountered in attempting to
determine hydrazine concentrations in the atmosphere.

b.   Experimental results

(1)   Hydrazine
        The change in the relative transmittance of the P(22) and
P(28) CO_2 lines after passage through the nitrogen-filled cell into which
1.6 $\mu\ell$ hydrazine was introduced is shown as a function of time in Fig. 12.
The extremely low vapor pressure of hydrazine ($\sim$ 12 Torr) results in a slow
evaporation rate within the limited cell volume and hence the long delay
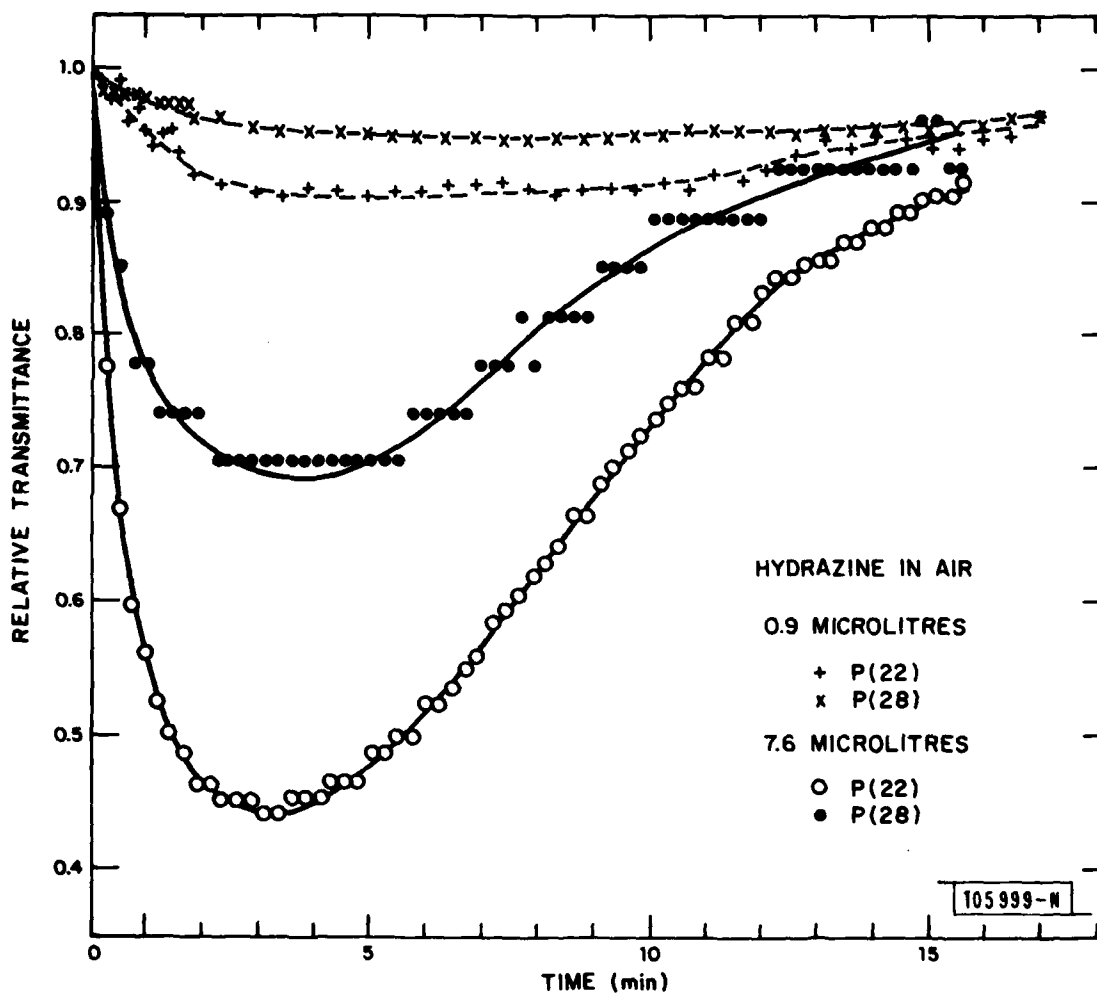observed in reaching the minimum transmittance level.

27

Fig. 13. Time variation of relative transmittance of 10.6-μm P(22) and 10.7-μm P(28) radiation through absorption cell containing air after insertion of 0.9 μℓ and 7.6 μℓ of liquid hydrazine.

Difficulties were experienced with the laser producing the P(28) transition line during the experiment so that the absorption by hydrazine of the P(28) line was terminated after about 35 min. By that time, the relative transmittance of the P(22) transition through the hydrazine vapor was within 4% of its subsequent equilibrium value. Taking an equivalent drop for the extrapolated P(28) line and assuming all the inserted liquid is present in the cell in the form of hydrazine vapor after equilibrium is achieved, the relative transmittance levels at their equilibrium values correspond to absorption coefficients of 5.27 and 2.26 $(cm\ atm)^{-1}$ for the P(22) and P(28) frequencies, respectively. These values are in close agreement with the published values[9] of 5.41 and 2.17 $(cm\ atm)^{-1}$

In order to simulate more closely the effect of remote sensing of hydrazine in the open atmosphere, the absorption of the P(22) and P(28) radiation was also measured after inserting hydrazine into the cell containing air instead of nitrogen. The resulting transmittance as a function of time is shown in Fig. 13 for the case of 0.9 μℓ of hydrazine and of 7.6 μℓ of hydrazine.

For the results shown in Fig. 13 obtained using 0.9 μℓ of hydrazine in air the maximum differential-absorption measured was almost an order of magnitude below the value obtained for hydrazine in nitrogen (Fig. 12). These results indicate that the quasi-equilibrium hydrazine vapor pressure was much smaller than in the case of the inert mixture. Given the combination of a slow vaporization rate and high oxidation rate for hydrazine, this result is not very surprising. It was observed that even after the absorption of the lines started to decrease, which occurred about 12 min. after the introduction of hydrazine into the cell, some liquid was still present in the cell.

The results shown in Fig. 13 obtained using 7.6 μℓ show the effect when an amount exceeding the saturation vapor pressure (~ 4.2 μℓ) is used. In this case, the relative transmittance reached a minimum value in less than 4 min. and returned to a near-normal value after about 15 min. The

maximum effective differential-absorption achieved under these conditions was approximately a factor of 4 below that predicted for saturated hydrazine vapor in the cell.

It should be noted that the decrease of hydrazine absorption observed in Fig. 13 was more rapid than anticipated on the basis of autoxidation studies.[13] In the open air, dispersive effects should lead to an even faster dissipation of absorption effects. These results indicate the need for a rapid measurement capability if the remote sensing of hydrazine is to be feasible.

(2) UDMH

The time variation of transmittance through the absorption cell after the insertion of 9 $\mu\ell$ of UDMH is shown in Fig. 14. These results are quite different than those shown in Fig. 5 for hydrazine. The vapor pressure of UDMH at room temperature ($\sim$ 165 Torr) is an order of magnitude greater than that of hydrazine and, as seen in Fig. 14, the relative transmittance of both the P(30) and the R(10) radiation reaches a minimum within a minute after the insertion of the UDMH into the cell.

The equilibrium values of the transmittance values shown in Fig. 14 correspond to absorption coefficients of 2.28 and 0.11 (cm atm)$^{-1}$ for the P(30) and R(10) frequencies, respectively. These values are considerably higher than the respective values of 1.45 and 0.05 (cm atm)$^{-1}$ obtained by Loper et al.[9] It is possible that wall reaction effects are responsible for these measured differences.

The experiment was repeated using air in the absorption cell in place of nitrogen and the results are shown in Fig. 15. They are almost identical with the results obtained in a nitrogen atmosphere, in agreement with studies[14,15] which indicate that UDMH is highly stable, even in an oxygen atmosphere.
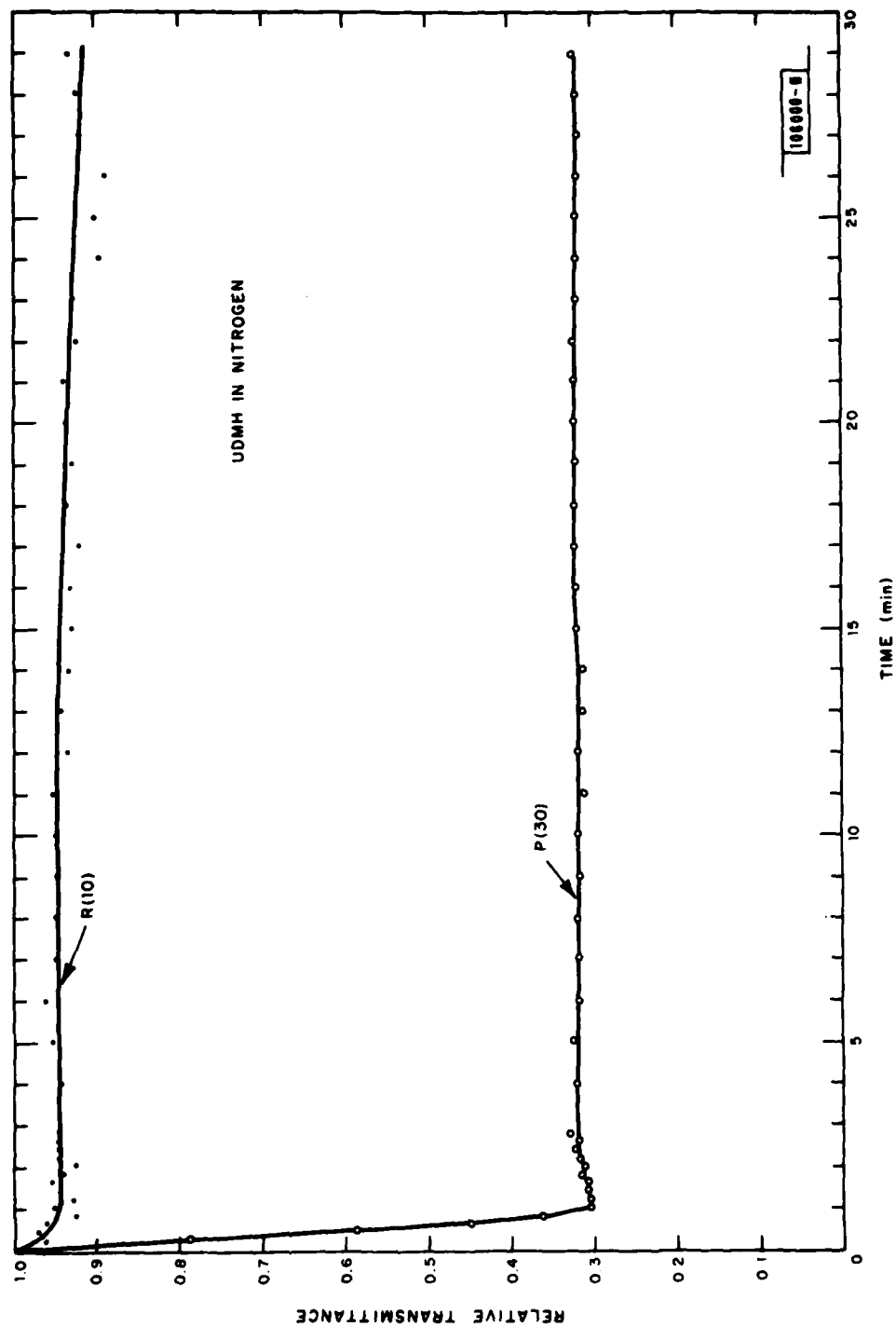
Fig. 14. Time variation of relative transmission of 10.7-μm P(30) and 10.3-μm R(10) radiation through absorption cell containing nitrogen after inserting 9 μℓ of liquid UDMH.
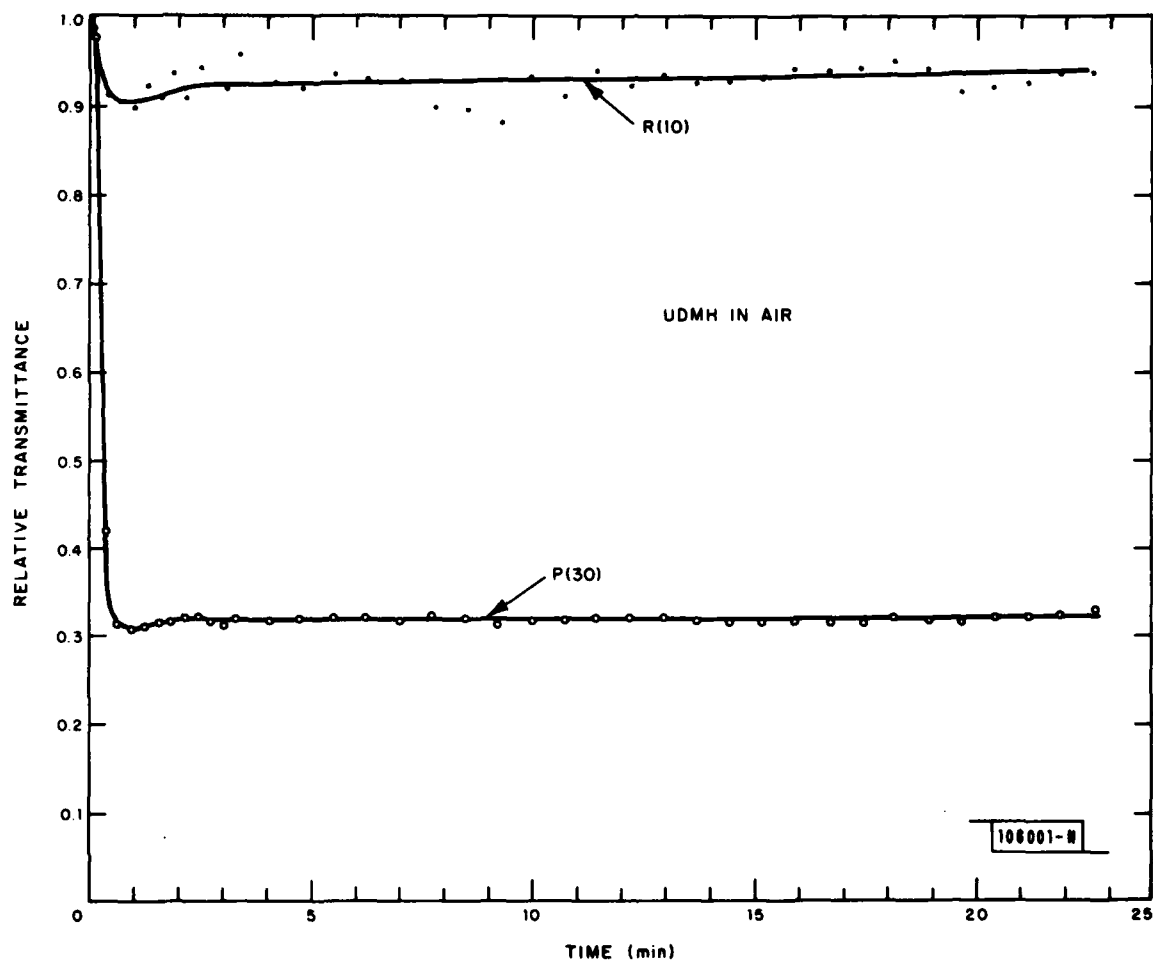
31

Fig. 15. Time variation of relative transmission of 10.7-μm P(30) and 10.3-μm R(10) radiation through absorption cell containing air after inserting 9 μℓ of liquid UDMH.

(3) MMH

Our absorption results for MMH are shown in Fig. 16. Mono-
methyl hydrazine has a vapor pressure of approximately 50 Torr at room
temperature and is much less volatile than UDMH. As seen in Fig. 16, after
inserting 9 μℓ of MMH into the nitrogen-containing absorption cell, 6 to 8
min. elapsed before the minimum transmittance level was reached. The MMH
absorption coefficients represented by the minimum relative transmittance
values correspond to 1.32 and 0.29 (cm atm)$^{-1}$ for the 9.28 μm R(18) and
10.18 μm R(30) transitions, respectively. These values compare favor-
ably with the published values[9] of 1.36 and 0.23 (cm atm)$^{-1}$ for these
lines.

The situation, however, is more complicated for MMH in an atmospheric
environment. Figure 17 shows the variation with time of the relative trans-
mittance of the same two transition lines after the insertion of 9 μℓ of
MMH into the air-filled absorption cell. In this case, the relative trans-
mittance at the R(30) frequency reached a minimum in slightly under 4 min.
and then increased significantly as the MMH was oxidized. The relative
transmittance at the R(18) frequency also decreased rapidly for the first
4 min. after MMH insertion, but then continued to decrease slowly. Appar-
ently the oxidation product of MMH is more absorbing at the R(18) frequency
than MMH itself. As a result, the differential-absorption of the two lines
reduced to zero after about 14 min. and then reversed sign.

To ascertain if ammonia, which is a known minor oxidation product of
MMH,[15,16] might be the source of the continued absorption of the 9.28-μm R(18)
line in Fig. 17, a similar experiment was performed with the 9.29-μm R(16)
line substituted for the R(18) transition. The ammonia absorption coef-
ficient at the R(16) transition frequency is over two orders of magnitude
greater than at the R(18) frequency. However, the effective absorption of
the MMH product at the R(16) frequency 30 min. after insertion of MMH into
the absorption cell was only 10% greater than the value obtained with
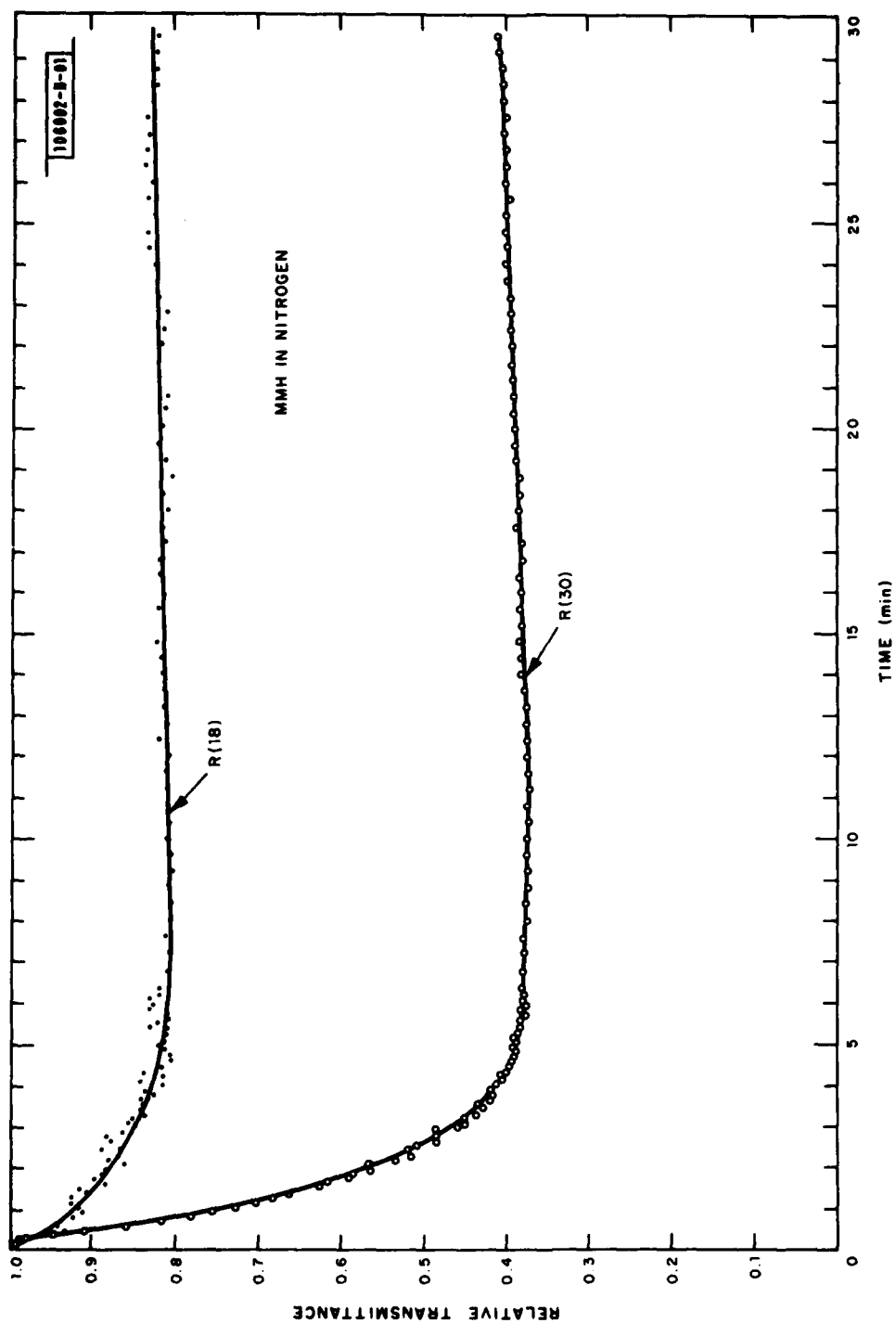
33

Fig. 16. Time variation of relative transmission of 10.2-μm R(30) and 9.3-μm R(18) radiation through absorption cell containing nitrogen after inserting 9 μℓ of liquid MMH.

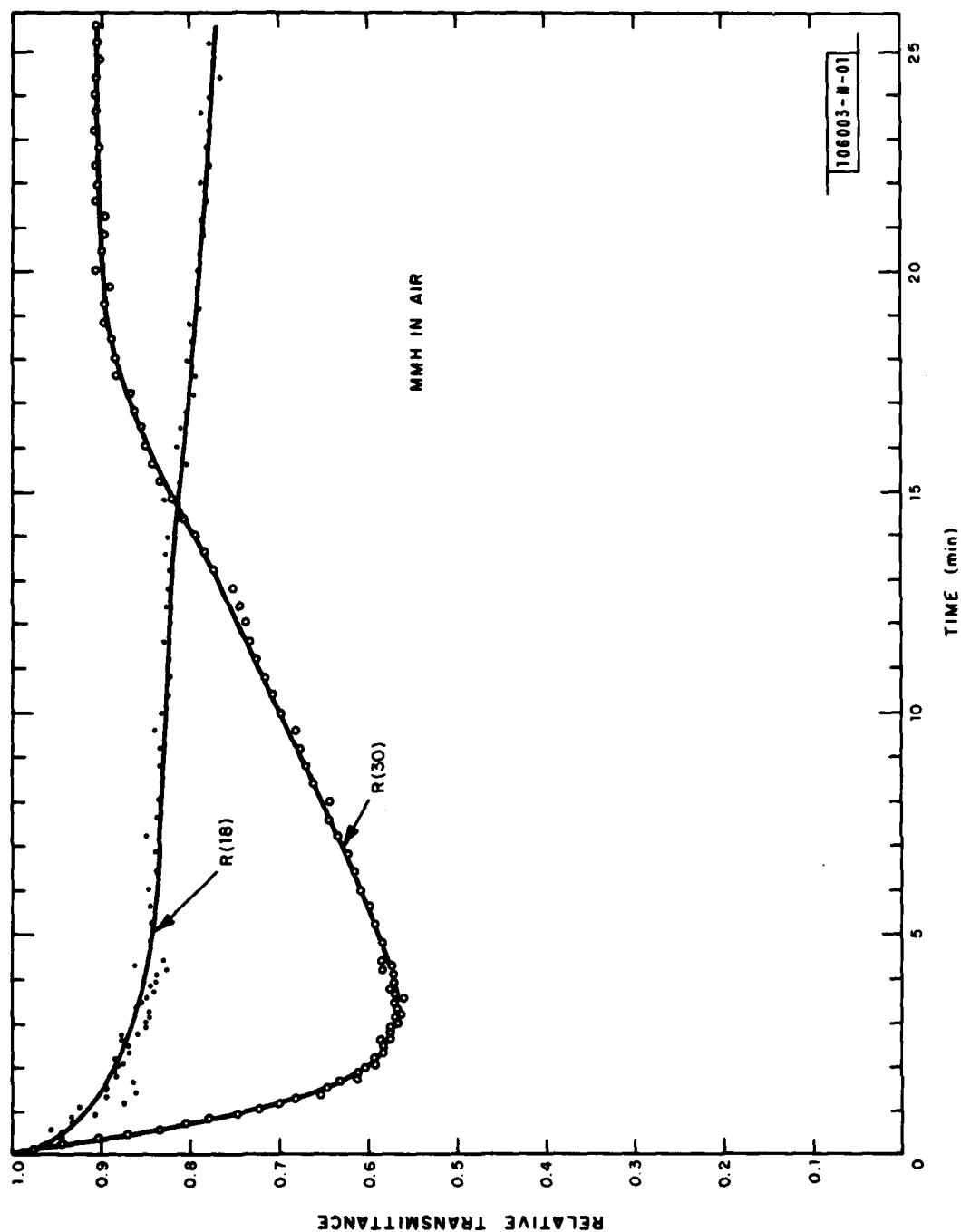MMH IN NITROGEN

R(18)

R(30)

RELATIVE TRANSMITTANCE

TIME (min)

Fig. 17. Time variation of relative transmission of 10.2-μm R(30) and 9.3-μm R(18) through absorption cell containing air after inserting 9 μℓ of liquid MMH.

35

the R(18) frequency. Ammonia can therefore be eliminated as the molecule
primarily responsible for the continued decrease of the R(18) transmittance.
Methanol is another known product of MMH decomposition with absorption in
the 9-10 μm region of the spectrum. However, this molecule can also be
eliminated, as its absorption coefficient is greater at the 10.18-μm R(30)
frequency than at the 9.28-μm R(18) frequency. It is possible that the
particular molecule causing the effect may be one of the formaldehydes
which form the bulk of the MMH oxidation products;[15] the formaldehydes
(-CHO) have weak absorption lines in the 10.3-12.8 μm region.

c.   Summary of results

Absorption coefficient measurements of hydrazine and MMH in a
nitrogen atmosphere, made with the CO_2 mini-TEA lasers used in the dual-
laser DIAL system were in excellent accord with literature values[9] obtained
using a low-pressure CO_2 laser. However, the values for UDMH indicated a
somewhat greater differential-absorption than predicted.

The effect of using air instead of nitrogen as the buffer gas in the
absorption cell led to markedly different results for hydrazine and MMH.
The rapid evaporation and stable optical absorption level observed after
inserting liquid UDMH into an air-filled cell indicate that an accurate
determination of the amount of UDMH introduced into the atmosphere may be
obtainable from a single temporal measurement. On the other hand, both
hydrazine and MMH exhibited considerable instability when introduced into
the air-filled cell, as evidenced by the rapid time variation of transmit-
tance through the cell. For the case of hydrazine it was found that after
inserting a known amount of liquid hydrazine into the air-containing cell,
the maximum hydrazine vapor levels achieved were much reduced from the
levels measured after insertion of the same amount of hydrazine into the
nitrogen-containing cell. The extent of the reduction was found to depend
upon the amount of hydrazine inserted, with the reduction greatest when the
amount is small.

For the case of liquid MMH insertion into the air-filled cell, the
time variation of transmittance through the cell is even more rapid than

was observed for hydrazine. An additional problem arises from the fact that an MMH oxidation product is absorbing at the low-absorption frequency chosen for our differential-absorption measurement. This interfering specie eventually causes the differential-absorption to change sign. Both ammonia and methanol have been eliminated as the interfering species responsible for this effect; it is probably due to one of the known[15] formaldehyde products.

6.4 Assessment of Results

The general agreement of the present absorption measurements with those of Loper et al.[9] indicates that the minimum detectable level for laser remote sensing of each of the hydrazines calculated in Section 6.2 are valid. On this basis, the laser remote sensing of UDMH, hydrazine, and MMH should be feasible at ranges of several kilometers for atmospheric concentrations of the order of tens of parts per billion.

The measurement of the concentration of the hydrazines in the ambient atmosphere, however, is complicated by their chemical reactivity and low vapor pressure. The results presented in this report indicate that while UDMH vapor concentration can be expected to remain stable (ignoring diffusion effects) for a significant period of time, the concentrations of hydrazine and MMH will vary rapidly. Under these circumstances the advantage of using a dual-laser DIAL system compared to a single-laser system for the remote sensing of the hydrazines is particularly marked since it measures the two frequencies almost simultaneously and has proven itself capable of taking differential-absorption measurements with a temporal resolution of the order of seconds.

VII. Summary and Recommendations

The research detailed in this report and the FY 79 final report[1] has demonstrated the capability of the laser remote sensing of atmospheric CO, NO, and C_2H_4 at concentrations of a few ppb and at ranges up to a few km.

The experimental results have determined the detection ranges and sensitivity of these measurements and have pointed to the need for a dual-laser DIAL system. Such a system is required to overcome the effects of atmospheric turbulence through the ability to "freeze" out such effects. It is anticipated that the use of this dual-laser DIAL system will greatly increase the measurement accuracy. Future experiments will quantify this.

The preliminary studies of the feasibility of laser remote sensing of hydrazine, UDMH, and MMH were encouraging. Laboratory results indicate that concentrations on the order of 10 ppb should be detectable at ranges up to several kilometers using our DIAL system. Investigations to experimentally verify these predictions are planned.

REFERENCES

1. A. Mooradian, D. K. Killinger and N. Menyuk, "Remote Sensing of Turbine Engine Gases," Final Report, Lincoln Laboratory, M.I.T., (30 September 1979), ESL-TR-80-09, DTIC AD-A084544/6.

2. D. K. Killinger, N. Menyuk, and W. E. DeFeo, Appl. Phys. Lett. 36, 402 (1980).

3. N. Menyuk, D. K. Killinger, and W. E. DeFeo, Appl. Opt. 19, 3282 (1980).

4. D. K. Killinger and N. Menyuk, Technical Digest, Topical Meeting on Coherent Laser Radar for Atmospheric Sensing, Paper ThC3, Aspen, Colorado, July 1980.

5. R. R. Patty, G. M. Russwurm, W. A. McClenny, and D. R. Morgan, Appl. Opt. 13, 2850 (1974).

6. A. Mayer, J. Comera, H. Charpentier, and C. Jaussaud, Appl. Opt. 17, 391 (1978) and 19, 1572 (1980).

7. R. A. McClatchey, R. W. Fenn, J. E. A. Selby, F. E. Volz, and J. S. Garing, "Optical Properties of the Atmosphere (Third Edition)," Report AFCRL-72-0497, Environmental Research Paper No. 411 (1972).

8. N. Menyuk and P. F. Moulton, Rev. Sci. Instr. 51, 216 (1980).

9. G. L. Loper, A. R. Calloway, M. A. Stamps, and J. A. Gelbwachs, Appl. Opt. 19, 2726 (1980).

10. R. J. Brewer and C. W. Bruce, Appl. Opt. 17, 3746 (1978).

11. S. T. Hong and A. Ishimaru, Radio Sci. 11, 551 (1976).

12. A. G. Kjelaas, P. E. Nordal, and A. Bjerkestrand, Appl. Opt. 17, 277 (1978).

13. G. L. Loper, "Gas Phase Kinetic Study of Air Oxidation of UDMH," Paper No. 12 in Proceedings of the Conference on Environmental Chemistry of Hydrazine Fuels, CEEDO-TR-78-14 (1978).

14. D. A. Stone, "The Autoxidation of Monomethylhydrazine Vapor," Report No. ESL-TR-79-10 (1979).

15. D. A. Stone, "The Autoxidation of Hydrazine and Unsymmetrical Dimethyl-hydrazine," Paper No. 13 in Proceedings of the Conference on Environmental Chemistry of Hydrazine Fuels, CEEDO-TR-78-14 (1978).

16. R. A. Saunders and J. T. Larkins, "Detection and Monitoring of Hydra-zine, Monomethylhydrazine and Their Decomposition Products," NRL Memorandum Report 3313/AD-A027 966 (1976).

APPENDIX

The following is a reprint of a journal article published
in Applied Optics, 1 October 1980, titled "Remote Sensing of NO
Using a Differential-Absorption LIDAR."

Remote sensing of NO using a differential absorption lidar

N. Menyuk, D. K. Killinger, and W. E. DeFeo

Single-ended remote sensing measurements of atmospheric NO have been made using differential absorption of frequency-doubled pulsed CO_2 laser radiation backscattered from topographic targets. Returns were obtained from targets at ranges out to 1.4 km, and significant NO concentrations above ambient were observed over a path which crossed a traffic roadway at a range of 0.5 km. In view of the severe atmospheric water vapor absorption in the spectral region containing the NO absorption band, the range dependence of the lidar returns was also measured in order to determine the differential absorption of the ambient atmosphere. The results differed significantly from those computed from atmospheric transmission data tapes.

Nitric oxide is a major constituent of auto exhaust emission and industrial stack effluence. It plays an important role in the production of photochemical smog and influences the global concentration of ozone in the atmosphere. Its detection by differential absorption techniques has recently been accomplished in a double-ended lidar system using a cw diode laser,[1] and with a cw CO laser[2] using spectral coincidences[3] between the fundamental 1–0 absorption band of NO and laser transitions of CO. These investigations were conducted using double-ended systems and clearly established the applicability of differential absorption for the remote sensing of NO in the atmosphere.

In this paper we describe single-ended differential absorption lidar (DIAL) measurements of NO in the atmosphere using frequency-doubled CO_2 laser radiation backscattered from topographic targets. Using spectral coincidences between the frequency-doubled CO_2 laser radiation and NO absorption lines[4] near 5.3 μm, signal returns were obtained from targets at ranges up to 1.4 km under high humidity conditions using direct detection. Significant concentrations of atmospheric NO (250 ± 40 ppb) above ambient were measured over a path which crossed a well-traveled roadway. We have also investigated the range dependence of the DIAL returns and have found that, under the conditions of our experiments, significant differences

exist between our differential absorption results and those computed from a modified HITRAN program using the AFGL atmospheric transmission data tapes.

The differential absorption lidar system used in our experiments has been described previously.[5] It uses a line-tunable high-repetition rate (>500-Hz) pulsed mini-TEA CO_2 laser[6] as the primary radiation source. The pulse length, after frequency doubling in a $CdGeAs_2$ crystal,[7] was 70 nsec, with a pulse energy near 0.5 mJ. Portions of the frequency-doubled radiation were split off to provide pulse energy normalization and an absorption calibration by passage through a 50-cm absorption cell containing 500 ppm of NO in argon at atmospheric pressure. Since nitric oxide reacts chemically with oxygen to form NO_2 it cannot be mixed with air in the cell. We used argon as the buffer gas after determining that its effect on the absorption coefficient of NO was similar to that of air. The bulk of the frequency-doubled laser beam was expanded to a 6-cm spot size and directed out a window of our remote sensing facility toward topographic targets; the window is ~20 m above the ground. The backscattered signals were collected by a 30-cm Cassegrain telescope and detected noncoherently by an InSb detector. The return and calibration signals were processed through gated boxcar integrators, normalized and recorded.

A determination was made of all coincidences[8] between the absorption line frequencies[9] of the fundamental 1–0 band of NO and doubled CO_2 laser frequencies,[10] where coincidence was defined as a frequency difference $\Delta\nu$, less than 0.1 cm^{-1}. Consideration of atmospheric transmission, NO absorption, and available CO_2 laser power eliminated all the coincidences except that between the frequency-doubled $P(24)$ CO_2 laser line of the 10.6-μm band and the $R(1/2)_{1/2}$ absorption line of NO. For this pair, $2\nu(CO_2)$ = 1881.098 cm^{-1}, $\nu(NO)$ = 1881.040 cm^{-1}, and $\Delta\nu$ = 0.058 cm^{-1}.

The authors are with MIT Lincoln Laboratory, Lexington, Massachusetts 02173.

42

An important consideration for the remote sensing of NO in the troposphere is that water vapor absorption is strong throughout the spectral region of the NO absorption band, including the region around 1881 cm^{-1}. This is seen in Fig. 1 which shows a computer-generated atmospheric transmission spectrum in this spectral region for a 3-km path at 296 K and 29% relative humidity.[11] The location of the doubled $P(24)$ coincident line is shown in Fig. 1 and is seen to lie in a small region of relatively high atmospheric transmission. The figure also indicates that the neighboring doubled $P(26)$ and $P(14)$ lines occur at frequencies with comparable transmission, so either can be used as the off-resonance line in differential absorption. The experiments described here were carried out at 293 K and 55% relative humidity, so the atmospheric transmissivity under the experimental conditions was significantly poorer than is indicated in Fig. 1.

To obtain a direct experimental determination of the sensitivity of our DIAL system for the measurement of NO in the atmosphere, a large tank of 60.5-cm diam × 104-cm length, with Mylar windows angled at 15° to avoid reflection effects, was filled with argon at atmospheric pressure and placed between our lidar system and a target consisting of foliage located 550 m from the laboratory. Upon insertion of a known amount of NO into the tank, the observed differential absorption signal agreed within 5% with the value obtained using the 50-cm laboratory absorption cell. These results indicated an overall system sensitivity of 40 ppb for the remote sensing of NO at a range of 550 m.

The average atmospheric NO concentration, N_a, as deduced from the differential absorption of the laser beams is given by

$$N_a = \frac{N_c L}{2R}\left[\frac{2(\beta_a' - \beta_a)R - \ln(P_a/P_a')}{-\ln(P_c/P_c')}\right], \qquad (1)$$

where N_c is the NO concentration in the absorption cell of length L, R is the distance to the target, P_a is the normalized on-resonance backscattered lidar signal, P_c is the normalized on-resonance absorption cell signal, and β_a is the atmospheric absorption coefficient at the resonance frequency in the absence of NO. The primes indicate the corresponding off-resonance values. Equation (1) is valid for $N_c \gg N_a$ such that $|L(\beta_c' - \beta_c)| \ll |\ln(P_c/P_c')|$; these conditions were met in our experiments.

The determination of NO concentration on the basis of Eq. (1) using differential absorption lidar returns from a single target requires an accurate knowledge of the difference in the atmospheric absorption, $\beta_a' - \beta_a$, at the different frequencies. Atmospheric absorption values at each frequency can be obtained from the AFGL atmospheric transmission data tapes[12] for known atmospheric conditions. However, since the computed values of β_a and β_a' at these frequencies are based on the sum of the theoretical contributions of a large number (~20–25) of absorption lines, small individual errors can result in a large overall discrepancy in $\beta_a' - \beta_a$.

To establish if the atmospheric absorption values obtained from the AFGL tapes might be sufficiently
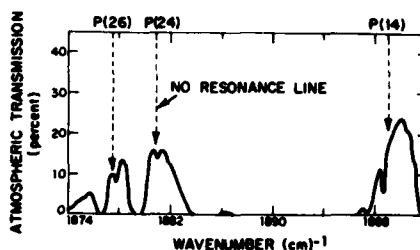

Fig. 1. Computer-generated atmospheric transmission curve for a 3-km path length at $T = 296$ K and 29% RH (Ref. 11). Also shown is the spectral location of the frequency-doubled CO_2 laser lines used in differential absorption experiments.
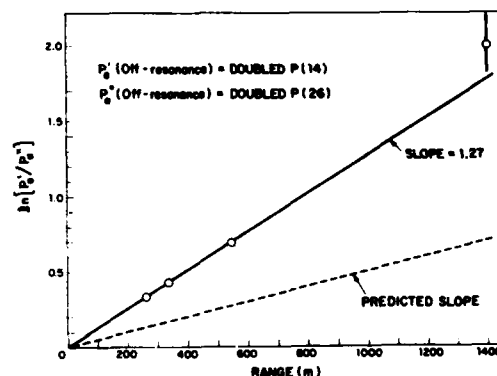

Fig. 2. Range dependence of the logarithmic ratio of return signals from topographic targets obtained using nonresonant frequencies. The dependence predicted using AFGL tapes is shown for comparison by the dashed line.

accurate for use in our experiments, we measured the lidar return signals from a number of targets at different ranges using two frequency-doubled CO_2 laser lines which are not resonant with NO absorption. In this case, the range dependence of the logarithmic ratio of the returns at the two frequencies is given by

$$\frac{d}{dR}[\ln(P_a'/P_a'')] = 2(\beta_a' - \beta_a''), \qquad (2)$$

where the primes and double primes refer to the two off-resonance frequencies. Equation (2) indicates that a plot of the logarithmic return ratio vs range should lie on a straight line passing through the origin, with a slope equal to twice the difference in the atmospheric absorption coefficients at the two frequencies. This experimental value can then be compared with the value computed on the basis of the AFGL tapes.

Using the frequency-doubled $P(14)$ and $P(26)$ CO_2 laser lines as the primed and double-primed frequencies, respectively, we obtained differential absorption returns from a series of targets at ranges from 0.25 to 1.4 km; our results are shown in Fig. 2. As seen in the figure, the measured logarithmic return ratio varies linearly with range, as predicted by Eq. (2). However, the

43

measured atmospheric absorption difference, $\beta_a' - \beta_a''$, is more than twice as large as the value predicted using the AFGL tapes. These results indicate that, under our experimental conditions, the predicted values of $\beta_a' - \beta_a''$ in Eq. (1) cannot be assumed to be sufficiently accurate to provide an NO concentration determination on the basis of lidar returns from a single target. This point will be discussed more fully below, after presenting further experimental results.

A range-dependent approach can be used to determine NO concentrations by measuring the differential lidar return from several targets using an off-resonance and an on-resonance laser line. Using Eq. (1), one obtains

$$\frac{d}{dR}[\ln(P_a/P_a')] = 2(\beta_a' - \beta_a)\frac{2N_a}{N_tL}\ln(P_t/P_t'), \quad (3)$$

which is valid for a constant ambient value of N_a. For this case, the logarithmic lidar return ratio vs range is again a straight line passing through the origin but with a slope dependent upon the ambient level of NO. The natural background level of NO is 0.2–2 ppb,[13] which would be undetectable in our system. However, significant increases above ambient due to localized emission will be distinguished by departure from the linear dependence of Eq. (3).

A set of differential absorption lidar returns were obtained from a series of targets using the frequency-doubled $P(24)$ and $P(26)$ lines as the on- and off-resonance lines, respectively. The ranges varied considerably, but the lines of sight to the various targets lay within an angular spread of $<4°$. The results are shown in Fig. 3. The two inner targets were removed from significant NO emission sources. The straight line joining these two targets passes through the origin and so defines the ambient extinction level as a function of range in accordance with Eq. (3). This level is shown as the solid line in Fig. 3. The resultant slope in this case also deviates sharply from that predicted on the basis of the tape-generated value assuming zero ambient NO, as shown in Fig. 3. This line cannot be brought into coincidence with the experimental line on the basis of the last term on the right-hand side of Eq. (3), since the presence of ambient NO would only increase the deviation.

The laser beam path to the target at 550 m in Fig. 3 crossed a traffic roadway at a height near 15 m. The return from this target indicates little NO concentration above ambient, suggesting that a height of 15 m is sufficient to reduce the NO content above a roadway to near the ambient value.

The path to the target at 480 m crossed the same traffic roadway but at a height of 3 m. The upper data point at this range was obtained immediately following the measurement at 550 m. The deviation of this point from the ambient extinction line is well beyond our experimental uncertainty and corresponds to an average NO concentration of 90 ppb over the laser beam path. Similar returns over the same path during a period of heavy traffic yielded average concentrations of NO up to 250 ppb, as indicated by the arrow and lower data
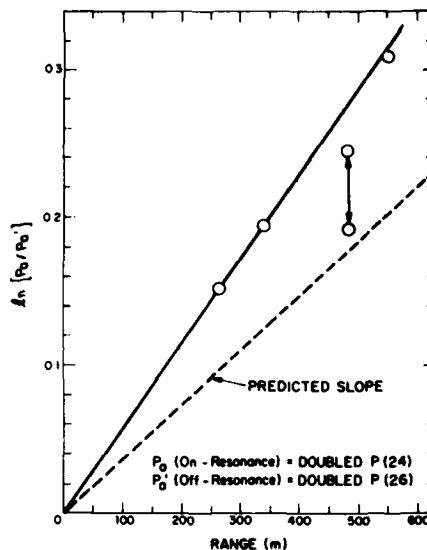
point. The rapid falloff of NO concentrations between heights of 3 and 15 m indicates a strong localization and hence a high concentration of NO in the immediate vicinity of the roadway. This is consistent with the rapid depletion by oxidation of NO in the atmosphere.

To further investigate the deviation of the measured differential absorption lidar returns from those predicted by the HITRAN program, a similar set of measurements was obtained using the frequency-doubled $P(24)$ and $P(14)$ CO_2 laser lines and targets removed from NO emission sources. The results are shown in Fig. 4. The linear dependence of the logarithmic return ratio with range is in accord with Eq. (3), and the slope of the resultant line is again seen to deviate significantly from that predicted on the basis of the tapes, assuming a zero ambient NO content. To bring the predicted line into coincidence with the experimentally determined line would require an ambient NO level near 800 ppb, which is more than 2 orders of magnitude above a reasonable ambient level. In addition, maximal contributions due to errors in the assumed water vapor content of the atmosphere correspond to less than one-tenth of the observed difference between the experimental and predicted results.
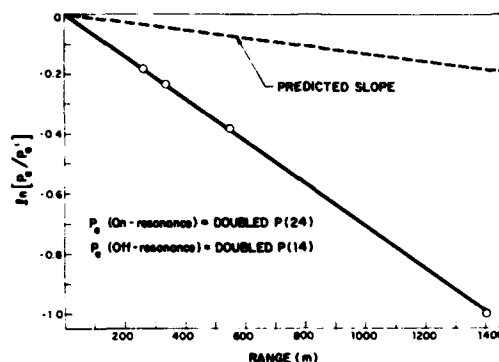
44

Fig. 4. Differential absorption return vs range with frequency-doubled $P(14)$ radiation as the nonresonant frequency source. The dependence predicted using AFGL tapes for zero ambient nitric oxide is shown by the dashed line.

In view of these differences, it is apparent that one cannot simply use values generated by the AFGL absorption line tapes to eliminate atmospheric background absorption effects. Our results indicate that such an approach would have led to large errors in the differential absorption of all three frequency pairs used in these experiments. There are several causes of these large discrepancies. The first, as noted previously, is the fact that the absorption coefficient at each frequency involves contributions from a large number of absorption lines. A significant contribution can come from the wings of these lines, where shape uncertainty is greatest. It should also be noted that the percentage errors in the individual values of β_a or β'_a may be fairly small and still lead to a large percentage error in $\beta'_a - \beta_a$. Second, discrepancies may be due to the laser source. The tape-generated values assume a single laser frequency for each laser line. However, TEA CO_2 lasers operating at or near atmospheric pressure generally operate on more than one longitudinal mode within a single line, with each mode radiating at a slightly different frequency; furthermore, there is a small degree of tunability within each CO_2 laser line. Under these circumstances, the accurate determination of the atmospheric absorption for a given experiment requires that the atmospheric absorption be measured at the same time as the pollutant concentration is being determined to ensure that both measurements are carried out at the same frequencies.

To do this and obtain an NO concentration determination from a single target requires a rather complex system. In addition to the simultaneous measurements presently being made of the lidar return and of absorption in the NO-containing calibration cell, an additional simultaneous set of measurements would be needed of absorption through a cell containing water vapor. Given the limited water vapor absorption under saturation conditions over short lengths at usable frequencies, this cell would have to be either an ultrasensitive spectrophone or a multipath absorption cell. The alternative of using multiple targets for the direct measurement of the differential absorption at the on- and off-resonance frequencies was therefore chosen as the simpler approach. However, we are presently constructing the cells for water vapor measurements, which will permit single-target NO concentration determination. It will also enable us to resolve the apparent discrepancies between our water vapor absorption measurements at the doubled CO_2 laser frequencies and the tape-generated values in a laboratory environment.

In conclusion, we have shown that frequency-doubled CO_2 laser radiation can be used for the single-ended remote sensing of atmospheric NO concentrations, even under conditions of relatively high atmospheric water-vapor content. Differential absorption lidar returns were obtained from topographic targets out to 1.4 km, which far exceeds the ranges previously reported for remote sensing of NO in direct detection systems. Our results also indicate that lidar returns from multiple targets can be used to measure local sources of NO even when the background atmospheric absorption coefficients at the individual laser frequencies are unknown.

Note Added: After submission of this paper, we became aware of another atmospheric transmission computer program devised by Thomas and Nordstrom.[14] Their program, like our HITRAN program, uses the AFGL data tapes. However, they use a different line-shape function, one in which the absorption

45

Frequency doubled laser lines	$\beta_a - \beta'_a$			
	Exp.	TN	LASER	HITRAN
$P(14)-P(26)$	0.635	0.565	0.30	0.25
$P(24)-P(14)$	−0.35	−0.224	−0.11 −0.07	
$P(24)-P(26)$	0.285	0.341	0.19	0.18

line is taken to be Lorentzian within 5 cm^{-1} of the absorption line center but is modified beyond 5 cm^{-1}. This contrasts with our HITRAN program, which assumes a Lorentzian line shape throughout. Thomas and Nordstrom used their program to calculate the values of the atmospheric extinction coefficients β_a under the conditions of our experiments (293 K, 55% RH) for the frequency-doubled $P(26)$, $P(24)$, and $P(14)$ CO$_2$ laser wavelengths and obtained values of 2.418, 2.077, and 1.853 km^{-1}, respectively. These are considerably higher than our HITRAN-calculated values of 1.20, 1.02, and 0.955 km^{-1}, respectively.

For completeness we contacted McClatchey and D'Agati who provided the equivalent set of values based on their LASER program,[15] which also uses the AFGL data tapes and assumes a Lorentzian absorption line shape. The extinction coefficients obtained from their program were 1.37, 1.18, and 1.07 km^{-1}, respectively, which are in close agreement with our results based on the HITRAN program.

The strong disagreement between the results of the Thomas-Nordstrom (TN) program and either the HITRAN or LASER program indicates that the absorption coefficients in this frequency region are strongly dependent upon the line shape in the wings of the absorption lines. Upon first consideration, given the large number of absorption lines involved at each of the frequencies, it would be reasonable to expect the modified wing shape to simply raise or lower an effective background (or virtual continuum) level and thus appear as an additive effect. Surprisingly, this is not the case. Instead, the effect is multiplicative, with a nearly constant ratio relating each of the equivalent extinction coefficients from the different programs. Further work will be required to clarify this point.

A comparison of the experimental values of $\beta'_a - \beta_a$, as described in this paper, with the values calculated by the different computer programs, is given in Table I. The values obtained by the TN program are seen to agree much more closely with our experimental results than those obtained with either the LASER or HITRAN program. The discrepancies that still exist between the experimental results and the TN values, however, correspond to an uncertainty in the reduced NO concentration of 150–350 ppb with an internal inconsistency of 200 ppb, which is much greater than our experimental uncertainty of 40 ppb or the anticipated ambient background concentration of NO ($\sim$2 ppb). Therefore, although use of the TN program markedly improves the

agreement with our experimental data, our results indicate that accurate evaluation of average NO concentration in the atmosphere still requires the simultaneous measurement of atmospheric absorption or the use of multiple targets.

References

1. E. D. Hinkley, Opt. Quantum Electron. 8, 155 (1976).
2. R. T. Menzies and M. S. Shumate, Appl. Opt. 15, 2080 (1976).
3. U. List, W. Hermann, W. Urban, and E. H. Fink, Appl. Phys. 19, 427 (1979).
4. R. T. Menzies, Appl. Opt. 10, 1532 (1971).
5. D. K. Killinger, N. Menyuk, and W. E. DeFeo, Appl. Phys. Lett. 36, 402 (1980).
6. N. Menyuk and P. F. Moulton, Rev. Sci. Instrum. 51, 216 (1980).
7. N. Menyuk, G. W. Iseler, and A. Mooradian, Appl. Phys. Lett. 29, 422 (1976).
8. A. Mooradian, D. K. Killinger, and N. Menyuk, MIT Lincoln Laboratory Report ESD-TR-79-319/ESL-TR-80-09 (1979).
9. A. Valentin, J. P. Boissy, P. Cardinet, A. Henry, D. W. Chen, and K. N. Rao, C. R. Acad. Sci. Ser. B: 283, 233 (1976).
10. M. A. Pollack, "Molecular Gas Lasers," in *Handbook of Lasers*, R. A. Pressley, Ed. (CRC Press, Cleveland, Ohio, 1971).
11. R. J. Nordstrom, J. H. Shaw, W. R. Skinner, J. G. Calvert, W. H. Chan, and W. M. Uselman, Environmental Science Research Laboratory Report EPA-600/3-77-026 (1977).
12. R. A. McClatchey, W. S. Benedict, S. A. Clough, D. E. Burch, R. F. Calfee, K. Fox, L. S. Rothman, and J. S Garing, "AFCRL Atmospheric Absorption Line Parameters Compilation," Environmental Research Paper 434, AFCRL-TR-73-0096 (Air Force Cambridge Research Laboratories, Bedford, Mass., Jan. 1973).
13. D. J. Kroon, J. Phys. E: 11, 497 (1978).
14. M. E. Thomas and R. J. Nordstrom, to be published.
15. R. A. McClatchey and A. P. D'Agati, Environmental Research Paper 622, AFGL-TR-78-0029 (1978).

REPORT DOCUMENTATION PAGE		READ INSTRUCTIONS BEFORE COMPLETING FORM
1. REPORT NUMBER ESD-TR-81-41 TR-81-16	2. GOVT ACCESSION NO. AD-A099638	3. RECIPIENT'S CATALOG NUMBER
4. TITLE (and Subtitle) Remote Sensing of Turbine Engine Gases		5. TYPE OF REPORT & PERIOD COVERED Final Report 1 October 1979 – 30 September 1980
		6. PERFORMING ORG. REPORT NUMBER
7. AUTHOR(s) Dennis K. Killinger, Norman Menyuk, Aram Mooradian		8. CONTRACT OR GRANT NUMBER(s) F19628-80-C-0002
9. PERFORMING ORGANIZATION NAME AND ADDRESS Lincoln Laboratory, M.I.T. P.O. Box 73 Lexington, MA 02173		10. PROGRAM ELEMENT, PROJECT, TASK AREA & WORK UNIT NUMBERS Program Element No. 62601F Project No. 1900
11. CONTROLLING OFFICE NAME AND ADDRESS Engineering and Services Laboratory Air Force Engineering and Services Center Tyndall AFB, FL 32403		12. REPORT DATE 30 September 1980
		13. NUMBER OF PAGES 52
14. MONITORING AGENCY NAME & ADDRESS (if different from Controlling Office) Electronic Systems Division Hanscom AFB Bedford, MA 01731		15. SECURITY CLASS. (of this report) Unclassified
		15a. DECLASSIFICATION DOWNGRADING SCHEDULE

16. DISTRIBUTION STATEMENT (of this Report)

Approved for public release; distribution unlimited.

17. DISTRIBUTION STATEMENT (of the abstract entered in Block 20, if different from Report)

18. SUPPLEMENTARY NOTES

None

19. KEY WORDS (Continue on reverse side if necessary and identify by block number)

laser remote sensing	mini-TEA CO_2 laser
turbine engine gases	LIDAR (DIAL) system
environmental monitoring	absorption measurements
tactical detection and	remote detection of CO
discrimination	

20. ABSTRACT (Continue on reverse side if necessary and identify by block number)

   This is the FY 80 final report for a laser remote sensing program designed to investigate remote sensing techniques for the detection of jet aircraft exhaust gases.

   The specific tasks which were performed consisted of the following: (1) continuation of feasibility demonstration of CO_2 TEA laser remote sensing system and the detection of NO and C_2H_4 in the atmosphere, (2) continuation of laboratory absorption measurements of CO, NO, and C_2H_4, (3) initial laboratory investigation of suitability of laser remote sensing of hydrazine, UDMH, and MMH, (4) implementation of digital data acquisition and processing system, and (5) preliminary development of dual-laser DIAL system.

201650

DATE
ILME